4D Cardiac Segmentation and Respiratory Motion Modeling of the Human Heart

Guillem Crosas Cano

Department of Electrical Engineering

Northeastern University

Universitat Politècnica de Catalunya

A thesis submitted for the degree of

Telecommunications Engineering Degree

2009 June

Advisor: Professor Dana Brooks

Day of the defense:

Signature from head of committee:

Abstract

Atrial Fibrillation (AF) is a growing problem in modern societies with an enormous impact in both short term quality of life and long term survival. A recently developed promising approach to cure AF uses radiofrequency (RF) ablation to carry out Pulmonary Vein Antrum Isolation (PVAI) to the heart. However, the lack of proper 3D surgery training, planning, and guidance makes surgery a very difficult task to the surgeons and therefore the risk for the patient increases.

Some work has been done developing automatic methods to segment and track the beating movement of the heart, but the purpose of this work is to add the respiratory motion to the existent models.

The reconstructed heart surface will serve as a virtual computer model for the 3D surgery training, planning and guidance.

To Andrea, Llum and Jaume

Acknowledgements

I would like to acknowledge all the people who have helped me realize this thesis. Specially, I want to thank my supervisors, Dr. Dana H. Brooks and Dr. Gilead Tadmor. They have been really helpful and have given plenty of good ideas during many interesting discussions. I am especially grateful because they always found a moment to help me and I have enjoyed my research with them.

I would also like to thank all the people of the Biomedical Image Processing group at Northeastern for all the help and interesting group meetings, and I want to specially thank Burak Erem for all the hours he spent with me discussing about my Thesis and other interesting topics.

This thesis was conducted in collaboration with the University of Utah. I would like to thank Dr. Rob MacLeod for providing us the datasets and for the helpful advice.

Finally, I would like to thank my friends, parents and girlfriend for all the support I've received from them during all the Thesis.

Contents

List of Figures

Chapter 1

Chapter 2

Chapter 3

CHAPTER 1: Introduction

1. Problem statement and challenges

Atrial fibrillation is the most common cardiac arrhythmia (abnormal heart rhythm) and involves the two upper chambers (atria) of the heart **[1]**. Its name comes from the fibrillating of the heart muscles of the atria, instead of a coordinated contraction. It can often be identified by taking a pulse and observing that the heartbeats don't occur at regular intervals. However, a conclusive indication of AF is the absence of P waves on an electrocardiogram (ECG), which are normally present when there is a coordinated atrial contraction at the beginning of each heart beat.

A recently developed promising approach to cure Atrial Fibrillation uses radiofrequency ablation to carry out pulmonary vein antrum isolation **[2]**. Unfortunately, because of significant clinical and technical challenges this approach is used only in a very small number of patients. The hypothesis of this research is that current and future magnetic resonance imaging will allow this technique to become the standard treatment for Atrial Fibrilation.

To perform radiofrequency ablation a physician guides a catheter with an electrode at its tip to the area of heart muscle where there is an accessory (extra) pathway. The catheter is guided with real-time, moving X-rays (fluoroscopy) displayed on a video screen. The procedure helps the doctor place the catheter at the exact site inside the heart where cells give off the electrical signals that stimulate the abnormal heart rhythm. Then painless radiofrequency energy (similar to microwave heat) is transmitted to the pathway. This destroys carefully selected heart muscle cells in a very small area (about 1/5 of an inch). That stops the area from conducting the extra impulses that caused the rapid heartbeats.

The first and most important problem when performing radiofrequency ablation is the lack of proper 3-D visualization when placing the catheter inside the heart. Those X-rays techniques are only in 2D, and some new and better techniques are needed. The second problem is the requirement to perform complex maneuvers, normally carried out in the open chest, inside the closed thoracic cavity. Finally, the current surgical guidance method can be improved, because the small field of view of the endoscope can be obstructed by blood or other substances.

The first step in our general project was done last year by Gerard Pons in his thesis **[3]**. He created a 4D Cardiac Segmentation and Motion Modeling of the heart, but only taking care of the beating of the heart. He reproduced the heart motion with respiratory-gated data, so the effect of the respiration into the heart motion was avoided.

Our aim with this project will be to study the respiratory motion of the heart, using both ECG-gated and ungated data to extract the needed information, in order to reproduce the respiratory motion of the heart. The future work will consist in use both techniques and create a complete model of the heart motion due to respiration and beating, that represent a 4D model so the surgeon has a reference within the anatomy of the heart that will help him navigate with the catheter in the closed thoracic cavity.

To achieve our goal, this project will consist in:

1) Study the respiratory cycle of the heart

2) Find a method to associate each image with a respiratory phase inside the cycle
3) Find the boundary of the heart in every MRI
4) Extract the 2D respiratory motion for all the slices
5) Create a 4D model of the heart using all the slices plus the respiratory phase

At the end of our project, a 4D model of the respiratory motion of the heart will be created, and we will be able to compare this movement with the beating movement of the heart. Having both models will allow future students to develop a complete model that incorporates both motions and creates a better tool for the radiofrequency ablation treatments.

Chapter 2 explains our work with ECG-gated data, our problems and results, while Chapter 3 describes the results with ungated data, the problems that this data represent, but the better results we get from it.

2. Previous work

Previous work

The respiratory motion of the heart has been studied from long time ago, but still now we don't have precise and exact information about it. The movement due to the respiration was first studied more than 30 years ago, when Dougherty studied the effects of respiration on electrocardiogram, and noted that the heart undergoes anatomic rotation in the frontal plan with respiration (**[4]** and **[5]**). The next step in respiratory motion study was done by Bogren, when he provided the first quantitative study of the respiratory motion of the heart **[6]**. In this study it was observed that the superior-inferior motion at the valve planes was half as much as the superior-inferior motion of the diaphragm, which averaged 15mm during normal respiration.

Years later, Wang used 2D MRI at multiple breath-hold levels to conclude that the primary motion of the heart was translation in the superior-inferior direction, and that this movement at the level of the coronary ostia was between 0.6 and 0.7 times the displacement of the diaphragm **[7]**.

The next step in respiratory motion was a 3D rigid body analysis of the motion of the heart presented by McLeish **[8]**. The idea was, obtaining 3D MRI datasets of the whole heart at multiple breath-hold levels, register them using image intensity method. McLeish reported rotations and translations for different patients and volunteers, but a use of a 6mm imaging slice thickness and a 180ms temporal resolution were insufficient for isolating the effects of cardiac motion from the respiratory analysis.

Previous project

In the introduction we mentioned Gerard Pons´s project **[3]**. Our project is the second step inside a global project that pretends to develop methods for automatically segmenting and tracking the heart in 4-D cardiac MRI datasets. The reconstructed heart surface will serve as a virtual computer model for the 3D surgery training, planning and guidance.

In the first step of this work (Gerard Pons's part), he outlined some of the methods proposed to solve the problem of cardiac segmentation. His method was based on an active contour model and a geometric post-processing of the segmentation. In other words, he generated a 4-D model of the heart so the surgeon had a reference within the anatomy of the heart that will help him navigate with the catheter in the closed thoracic cavity. The approach consisted in:

Pre-operative stage:

1. Find the boundary of the heart in a dataset of 4D- MRI images with minimal user intervention.

2. Render the surface that will model the beating heart.

3. Parameterize this set of volumes, i.e. describe the set of volumes as a set of coefficients or numbers.

Operative stage:

4. Find the boundary of the 2D + time imaging that is available during surgery.

5. Parameterize these boundaries as was done with the 4D model.

6. Find the exact location of the 2D images in the 4D model, i.e register the operative imaging with the pre-operative model.

7. Once we have the parameterized 4D model on one hand and the parameterized contours on the other, we will compare this set of parameters and thus reducing the complexity of the problem.

At the point where Gerard Pons's Thesis finishes is where our Thesis begins, adding the respiratory information to find a complete method to recreate the motion of the heart due to both respiration and beating.

3. Anatomy of the heartbeat and of respiration

Some biological background is needed to understand the respiratory motion. It is important to learn why the heart is affected by the lungs and it is also important to understand how and why atrial fibrillation is produced. More information can be found in **[9]**, **[10]**, **[11]** and **[12]**.

The heart: Anatomy and physiology

Structure of the heart

The human heart is located in the center of the thoracic cavity between the two lungs, lying on the thoracic face of the diaphragm.

The right heart is composed by the right atrium (RA) separated from the right ventricle (RV) by the tricuspid valve and the RV is separated from the pulmonary artery by the pulmonary valve.

The left heart, much muscular and thick than the right heart, is composed by the left atrium (LA) and the left ventricle (LV) separated from the mitral valve, and the Aortic semilunar valve that separates the LV form the Aortic artery.

Unoxygenated blood comes from two major veins, Inferior Vena Cava and Superior Vena Cava, to the RA. When the pressure in the RV is greater than the pressure in the RA, the tricuspide valve is shut and the blood fills the RA. When the RV pressure decreases because of its relaxation, the pressure difference causes flow from the right atrium to the right ventricle, first passively and then actively as a result of RA contraction, which opens the tricuspide valve. When the RV is absolutely filled and its pressure is higher than the pulmonary artery pressure, the mitral valve is shut and the pulmonary valve is opened and the contraction of the ventricle causes the blood flow through the pulmonary arteries.

After the blood is oxygenated in the lungs, it arrives to the LA where the same circuit is done, but with higher pressures. The LA collect the blood from the lungs, it flows through the mitral valve to the LV. There are three papillary muscles which will help open and keep opened the Aortic valve. The LV generates a great pressure in order to overcome the systemic pressure, which is higher than the pulmonary system pressure.

Physiology

The heart is composed primarily of muscle tissue, but these contractile cells (myocardiocyte) have different characteristics than the skeletal muscle of the skeleton system with voluntary control, or the smooth muscle of the vascular system, which controls the blood flow through the body. Nevertheless there are other noncontractile autorhythmic fibers that form a specialized conducting system that rapidly transmits action potentials through the heart.

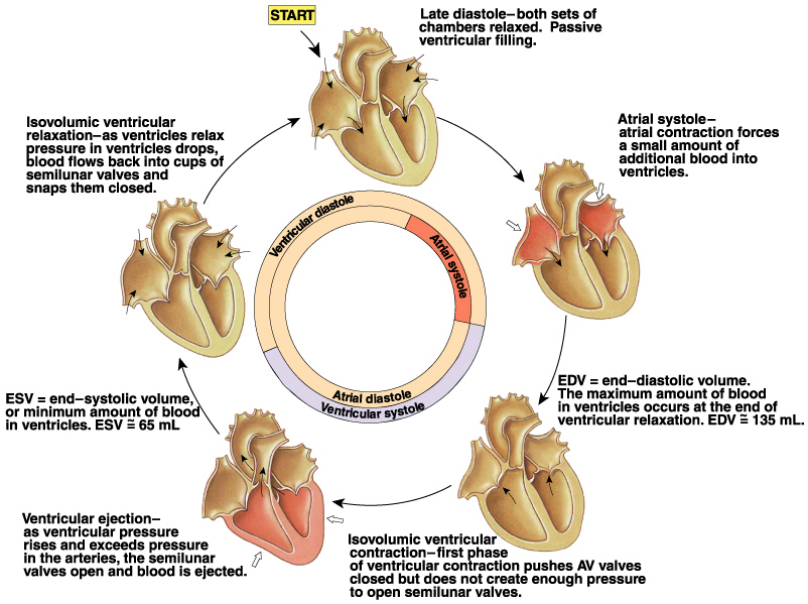

Figure 3.1. Physiology of the cardiac cycle

The initiation of myocardial contraction starts in the atria, in the sinoatrial node, nestled in the upper of the RA. The action potential generated by this node, spread throughout the atria primarily by cell-to-cell conduction and intermodal ways. As the wave of action potentials depolarizes the atrial muscle, the cardiomyocyte contract by a process termed excitation-contracion coupling. Normally the only pathway available for action potentials to enter the ventricles is through a specialized region of cells called atrioventricular node and located in the inferior-posterior region of the interatrial septum. The AV node slows the impulse conduction considerably thereby allowing sufficient time for complete atrial depolarization and contraction (systole) prior to ventricular depolarization and contraction.

The impulse then enters the ventricle at the Bundle of Hiss and then follows the left and right bundle branches of Hiss along the interventricular septum. These fibers conduct the impulses at a very rapid velocity. The bundle branches then divide into an extensive system of Purkinge fibers that conduct the impulse at high velocity trough the ventricles. This results in rapid depolarization of ventricular myocites through both ventricles

The conduction system within the heart is very important because it permits a rapid and organized depolarization of ventricular myocytes that is necessary for the efficient generation of pressure during systole.

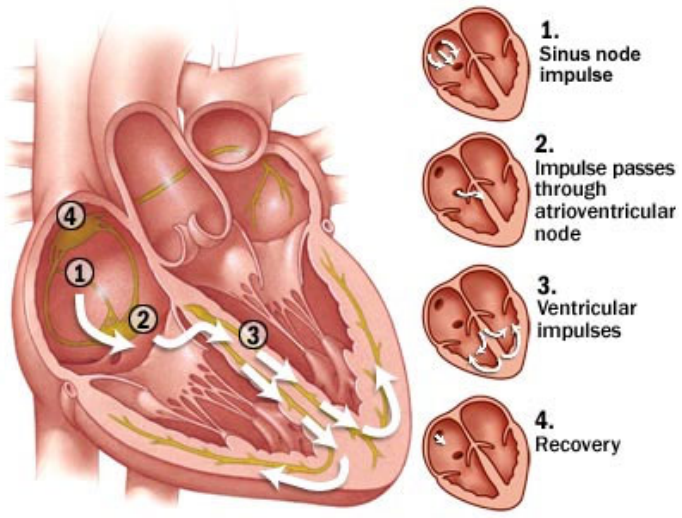

Figure 3.2. Electrical conduction throughout the heart

The electrical impulses throughout the heart are influenced by autonomic nerve activity. This control is most apparent at the AV node. The normal cardiac rate is about 60-100 heartbeat per minute. It can change with the autonomic activity control.

Sympathetic activation increases conduction velocity in the AV node by increasing the rate of depolarization of the action potentials, reducing the time between atrial and ventricular contraction. Parasypathetic or vagal activation decreases conduction velocity at AV node.

The action potential that triggers the heartbeat is generated within the heart itself. Motor nerves (of the autonomic nervous system) do run to the heart, but their effect is simply to modulate - increase or decrease - the intrinsic rate and the strength of the heartbeat. Even if the nerves are destroyed (as they are in a transplanted heart), the heart continues to beat.

The myocardial cells have five elemental properties, some of them are exclusives.

1. Excitability: The capacity of respond to a stimulus. The minimum intensity is called “excitation threshold”. The response of the myocardic fibers is the contraction.
2. Automatism: There are some cardiac cells capable of exciting without an external stimulus. The cellular groups with this capacity are called “natural pacemaker”. In mammal and human, the principal pacemaker is the sinoatrial node, although other structures (Hiss bundle and its branches) can do it too but slowly.
3. Conductivity: It is the property in which the electric excitation is transmited from a miocardic cell to the adjacent one. The conduction velocity depends on the cellular groups and the way of propagation.
4. Refractarity: This is a common property of all cardiac cells. After an exitation, exist an interval of time when the fiber is unable to respond to a new stimulus, regardless of its intensity (Absolute

Refractary Period). After this interval and with an stimulus with an intensity superior of the threshold, it can be obtained the cell excitation. (Relative refractary period)

5. Contractility: The heart is an electro-mecanic system, if dissociation exists, it does not work.

Biomechanics of the lung

Structure of Respiratory system

The respiratory system consists in the following structures:

- Airways: Tubes that carry air between environment and alveoli (from trachea through right and left bronchi, they are made of rigid cartilage, and the bronchi branch into bronchioles made of smooth muscle).
- Alveoli: Clusters of thin walled, inflatable, grapelike sacs at the terminal branches of the bronchioles, surrounded by pulmonary capillaries.
- Lungs and Chest cavity: The two lungs are supplied each by one of the bronchi. Lungs occupy most of chest cavity and the diaphragm forms the floor. Exists a pleural sac that separates each lung from the thoracic wall and other structures this pleural sac contains intrapleural fluid, allowing a good slide

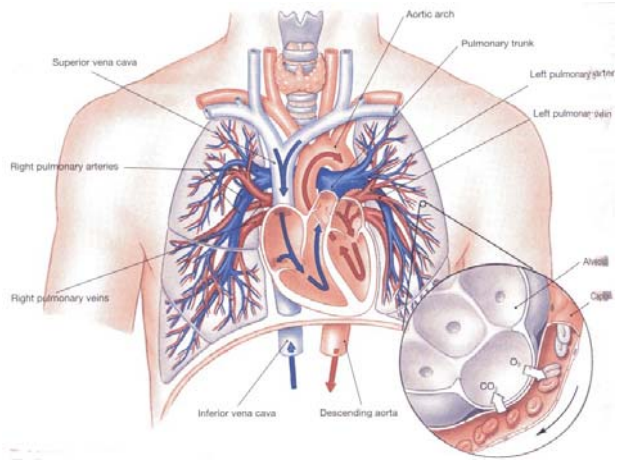

Figure 3.3. The human lung

Pressure considerations and statics of the lung

Air moves from a region of high pressure to low pressure; it flows down a pressure gradient. Air flows in and out of the lungs by reversing pressure gradients between lungs and environment.

The statics of the lung are a result of the trend of the lung tissues toward the retraction, and the thoracic walls toward the expansion.

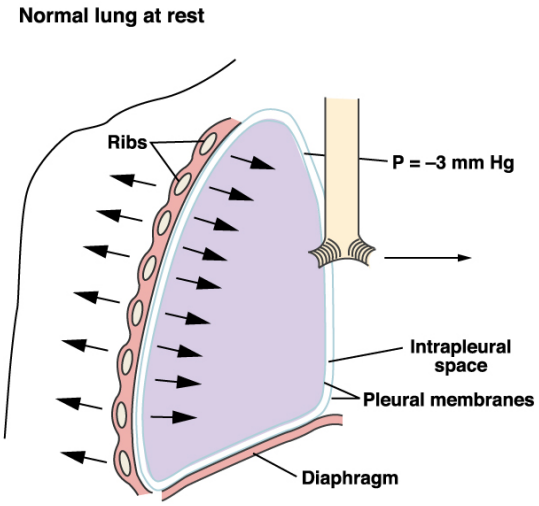

Figure 3.4. Physiology of the respiration

There are some important pressures related to respiration to consider:

a. Atmospheric (barometric) pressure: pressure exerted by weight of air in atmosphere on objects on earth's surface.
b. Intra-alveolar pressure (sometimes called intrapulmonary pressure) is the pressure within the alveoli.
c. Intrapleural pressure (also called intrathoracic pressure) is the pressure exerted outside the lungs within the thoracic cavity.
d. The intrapleural pressure is 756 mm Hg and the intra-alveolar pressure is 760 mm Hg when equilibrated with atmospheric pressure. This transmural pressure gradient across the lung wall is crucial in expanding the lung to fill the chest cavity.
e. Although elastic lungs 'want' to collapse, they don't because of this transmural pressure gradient

Respiratory Cycle

Respiration works by changing the volume of the chest cavity. Before the start of inspiration, respiratory muscles are relaxed, the intra-alveolar pressure is the same as the atmospheric pressure, and no air is flowing.

At onset of inspiration, inspiratory muscles (primarily the diaphragm) contract, this results in enlargement of the thoracic cavity. As the thoracic cavity enlarges, the lungs are forced to expand to fill the larger cavity.

Because the intra-alveolar pressure is less than atmospheric pressure, air follows its pressure gradient and flows into the lungs until no further gradient exists. Therefore, lung expansion is not caused by movement of air into the lungs.

At the end of inspiration, the inspiratory muscles relax, the chest cavity returns to original size, and the lungs return to original size. Although at rest expiration is a passive process, during exercise it is an active process and expiratory muscles (primarily abdominal muscles) contract to decrease the size of the chest cavity during expiration.

Cardio respiratory system

As we have mentioned, both systems (cardio circulatory and respiratory) are intimately related, physiologic and anatomically. Thereby, the movement of one organ may disturb the other. During the inspiration there is an increase of the cardiac frequency because the heart can't expand at all and the diastolic phase gets shorter. The opposite happens during the expiration.

Arrhythmias and ablation

We define arrhythmias as an alteration of the coordinate heart rhythm. It can occur when we have a too fast rhythm (tachycardia), too slow (bradycardia) or the frequency of the atrial and ventricular beats are different.This is a very prevalent disease, such as 14 million people in the USA. The most common disorders are atrial fibrillation and flutter. The incidence is highly related to age and presence of underlying heart disease.

The lack of oxygen of cardiac cells caused by coronary artery disease is a frequent cause of arrhythmia. This cells become depolarized, which lead to altered impulse formation and or altered impulse conduction, thereby exists an abnormal generation of action potentials at sites other than the SA node (ectopic focus). This altered impulse conduction can be associated with complete or partial block of electrical conduction.

Other causes of arrhythmias are changes in cardiac structure that accompany heart failure (e.g. dilated or hypertrophied cardiac chambers), different types of drugs (including antiarrhythmic drugs) and electrolyte disturbances (primarily potassium and calcium).

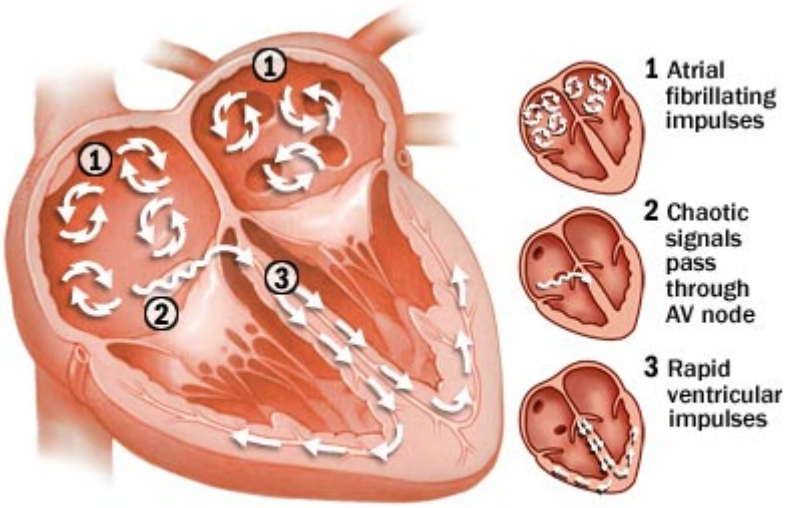

Figure 3.5. Electrical conduction during atrial fibrillation

All these conclude in a disorganized contraction of the four heart chambers that leads to a bad pumping function. The blood does not arrive regularly to the tissues.

Not all the arrhythmias require treatment; it depends on the hemodynamic repercussion. When they need treatment, the first option is the antiarrhytmic drugs. There are different groups depending in their mechanisms of action. Another option is the electrical cardioversion, and the goal of this thesis, the radiofrequency ablation therapy. In the atrial fibrillation, the most common indication of this technique, the best results have been obtained when the automatic foci are located in the pulmonary veins. While ablation of these foci is possible, the procedure can result in pulmonary vein stenosis, pulmonary hypertension, and stroke. In order to improve the results, technologic advances are necessary.

4. Background theory

Some background theory is needed before studying the different data. Spherical harmonics will be used at the end of the Thesis to represent the reproduced heart. It is a great solution to smooth the heart and at the same time to express its surface with a small number of coefficients. We will see in this chapter how the spherical harmonics are used, and at the same time how the resultant heart can be sliced to find its cuts with different planes.

Spherical Harmonics

If we have segmented the different frames and slices of the heart motion, we have a high amount of points to represent. In order to make it faster and because of the spherical shape of the heart, our objective is to represent the heart with Spherical Harmonic Coordinates. Examples of previous work in this field can be seen in **[13]**, **[14]**, **[15]** and **[16]**.

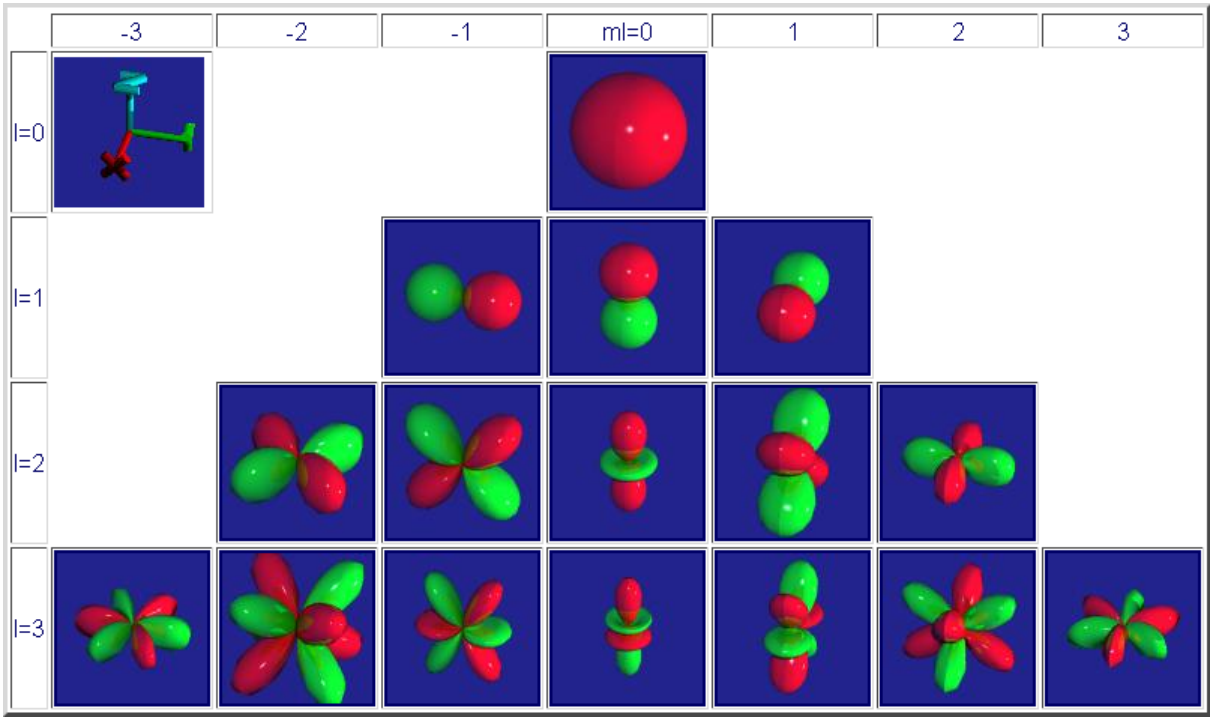

Figure 4.1. First spherical harmonics

Spherical Harmonic theory

The Spherical Harmonics are defined as the everywhere regular eigenfunctions of the spherical Laplace operator **[17]**. These functions constitute a complete orthonormal system of the space of integrable functions on the sphere.

The Laplace equation in spherical coordinates is:

$$\nabla^2 f = \frac{1}{r^2}\frac{\partial}{\partial r}\left(r^2\frac{\partial f}{\partial r}\right) + \frac{1}{r^2\sin\theta}\frac{\partial}{\partial\theta}\left(\sin\theta\frac{\partial f}{\partial\theta}\right) + \frac{1}{r^2\sin^2\theta}\frac{\partial^2 f}{\partial\varphi^2} = 0$$

And after solving this equation, the resultant differential equations solution can be shown as:

$$Y_\ell^m(\theta,\varphi) = \sqrt{\frac{(2\ell+1)}{4\pi}\frac{(\ell-m)!}{(\ell+m)!}}\, P_\ell^m(\cos\theta)\, e^{im\varphi}$$

Where Y_l^m is the spherical harmonic function of degree l and order m and P_l^m is the associated Legendre Function,

$$P_\ell^{(m)}(x) = (-1)^m\ (1-x^2)^{m/2}\ \frac{d^m}{dx^m}\left(P_\ell(x)\right)$$

The spherical harmonics form a complete set of orthonormal functions and thus form a vector space analogous to unit basis vectors. On the unit sphere, any square-integrable function can consequently be expanded as a linear combination of these:

$$f(\theta,\varphi) = \sum_{\ell=0}^{\infty}\sum_{m=-\ell}^{\ell} f_\ell^m\, Y_\ell^m(\theta,\varphi).$$

In our particular case, $f(\theta,\varphi)$ will be the radius of the heart for every θ and φ.

Given a set of points of the heart, how can we get these functions to represent the heart with only a few coefficients?

We can use all our data to find Y_l^m for all m and l, but the expression to find f_l^m needs a continuous surface to be integrated and we only have non-continuously spaced samples of this surface.

$$f_\ell^m = \int_\Omega f(\theta,\varphi)\, Y_\ell^{m*}(\theta,\varphi)d\Omega = \int_0^{2\pi} d\varphi \int_0^{\pi} d\theta \sin\theta f(\theta,\varphi) Y_\ell^{m*}(\theta,\varphi)$$

So we are obligated to find f_l^m with other techniques.

Spherical Harmonics applied to our problem

Our method to represent the heart surface with spherical coordinates is based in the previous formula, where the radius can be expressed as a function of θ and φ.

$$rad(\theta,\varphi) = \sum_{l=0}^{l=order}\ \sum_{m=-l}^{m=l} coef_l^m Y_l^m(\theta,\varphi)$$

where the *coef* are the numbers that will represent our heart. Notice that these *coef* do not depend of θ or φ, so they are generic.

To find the coefficients to represent the heart we will use a data of 73 points per 20 slices, that is 1460 points that represent the following heart:

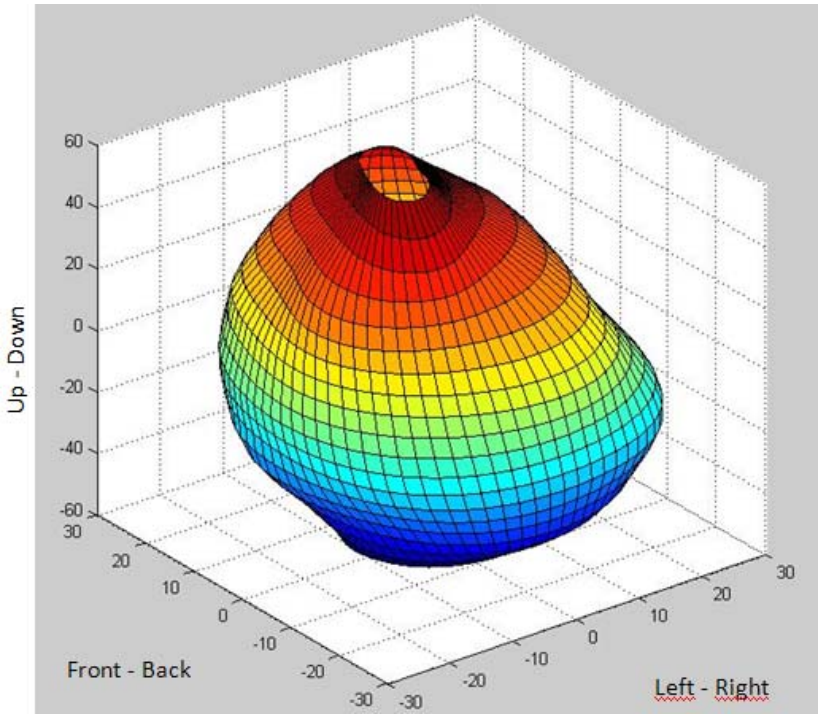

Figure 4.2. Original heart surface

With this points we will create one vector with all the radiuses $\boldsymbol{r}$, and a matrix with the values of the Y_l^m for all the θ and φ. With the previous notation we can express this sum as a matrix product, where we would like to have one coefficient vector and one Y matrix with all the values of the spherical functions.

$$\boldsymbol{r} = \boldsymbol{coef} * Y$$

Where

$$\boldsymbol{r} = [r_1 \quad r_2 \quad r_3 \quad r_4 \quad . \quad . \quad .]$$

and

$$Y = \begin{bmatrix} Y_0^{0(1)} & Y_0^{0(2)} & Y_1^{3(3)} & \dots & Y_0^{0(4)} & Y_0^{0(5)} & Y_0^{0(6)} & \dots \\ Y_0^{1(1)} & Y_0^{1(2)} & Y_1^{3(3)} & \dots & Y_0^{1(4)} & Y_0^{1(5)} & Y_0^{1(6)} & \dots \\ Y_1^{1(1)} & Y_1^{1(2)} & Y_1^{3(3)} & \dots & Y_1^{1(4)} & Y_1^{1(5)} & Y_1^{1(6)} & \dots \\ \dots & \dots & \dots & \dots & \dots & \dots & \dots & \dots \end{bmatrix}$$

In which every column contains all the values of Y_l^m for a given θ and φ. Due to the order of the rows, we can express the sum as a matrix product, and we can solve it easily.

So with this notation, the vector we need to find can be expressed as

$$\boldsymbol{coef} = \boldsymbol{r} * Y^{-1}$$

But as our matrix Y is not invertible, we have to use a numeric approach to solve this equation. The method we will use is to minimize the 2-norm of $\boldsymbol{r} - \boldsymbol{coef} * Y$, what means find the values of $\boldsymbol{r}$ that minimize this equation.

$$\| \boldsymbol{r} - \boldsymbol{coef} * \boldsymbol{Y} \|_2$$

Once we have found the coefficients, we can easily calculate every radius given any θ and φ, which means that now we have a continuous function for our heart surface.

$$\boldsymbol{r} = \boldsymbol{m} * \boldsymbol{y}$$

Where $\boldsymbol{y}$ is the equivalent to a column in the matrix Y but with the new θ and φ.

The next step will be to find the adequate order for our functions. Increasing the order creates more coefficients and if we use an order too high, it can present bad results.

Results of the spherical harmonics

Changing the order of the algorithm means changing the number of coefficients we are using, and the number of basis functions we are using to represent our surface.

The first attempt we can make is using a few number of coefficients (16) and see how far we are from the original heart.

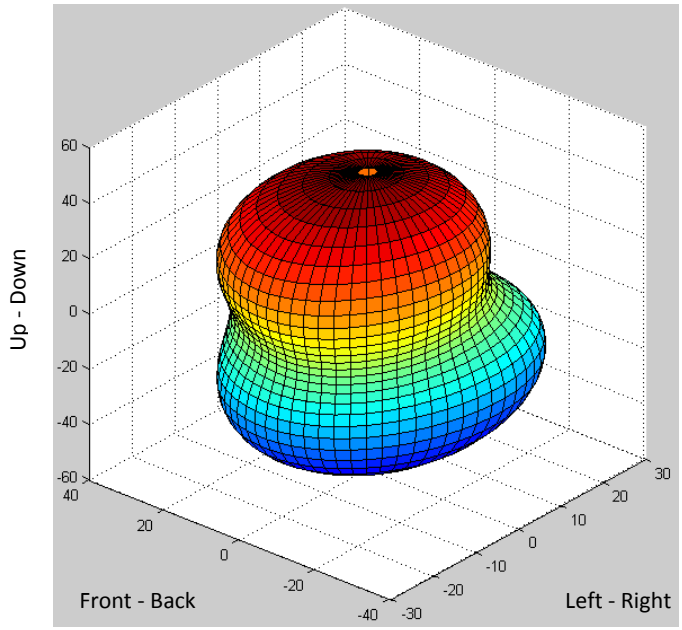

Figure 4.3. Heart surface reproduction with only 16 coefficients

We can appreciate that the resultant surface is very different from the original one (see fig 4.2). To quantify this difference, we can see the difference of volume between the original heart and the one created with the spherical harmonics.

In the next table we can see the errors using different orders in the algorithm:

Order	Coefficients	Error	Surface
Original	-	-	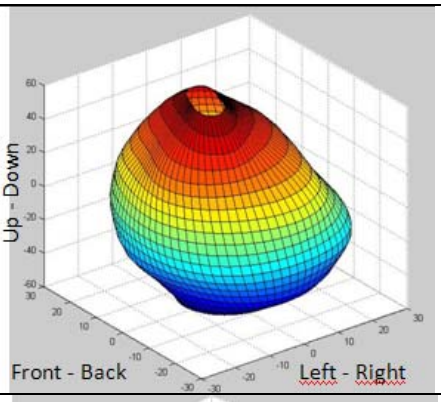
3	16	8.3%	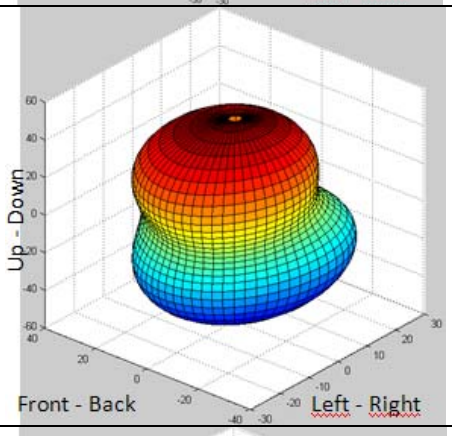
4	25	4.05%	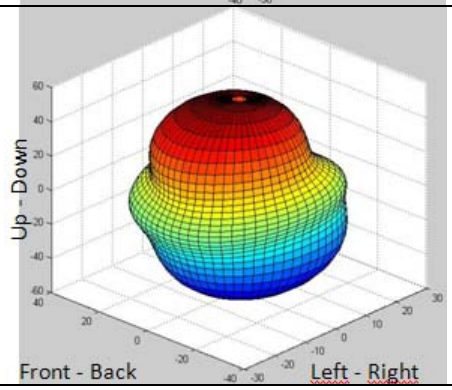

5	36	3.81%	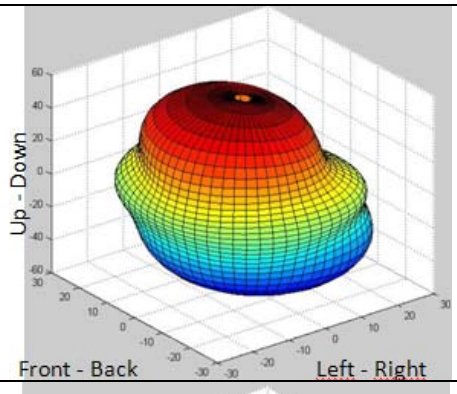
6	49	2.55%	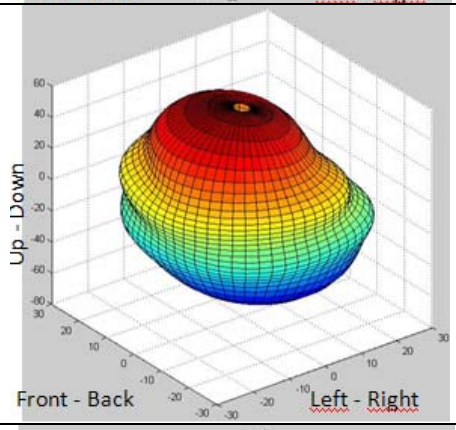
7	64	2.33%	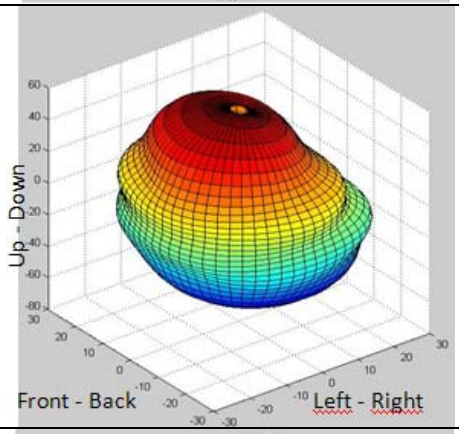
8	81	1.86%	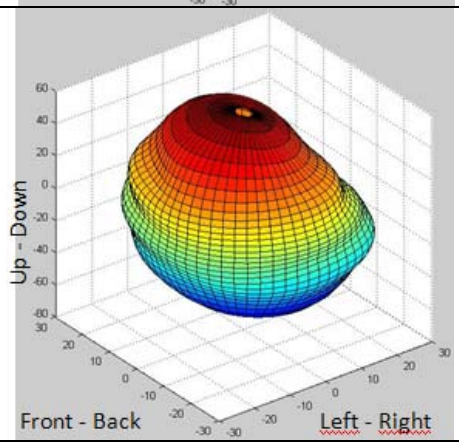

9	100	1.58%	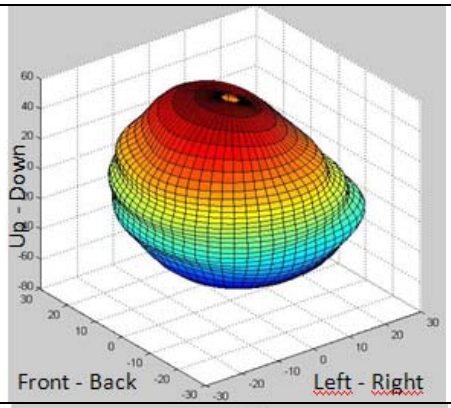
10	121	1.39%	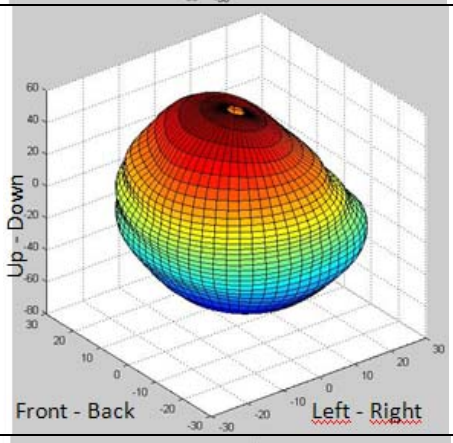
11	144	1.1%	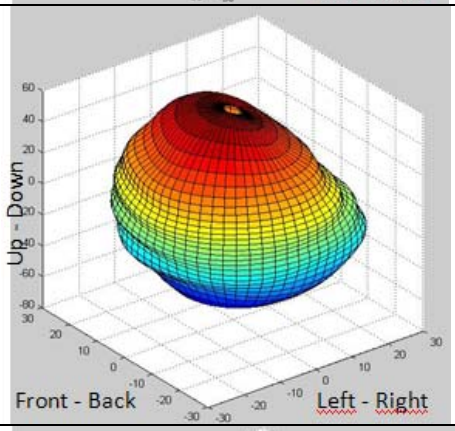
12	169	0.95%	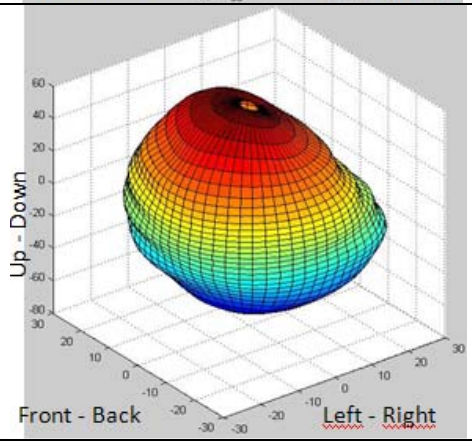

13	196	0.73%	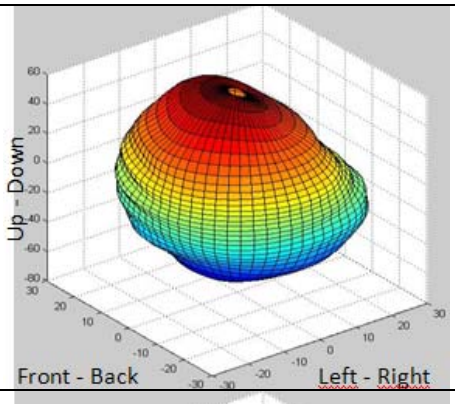
14	225	0.65%	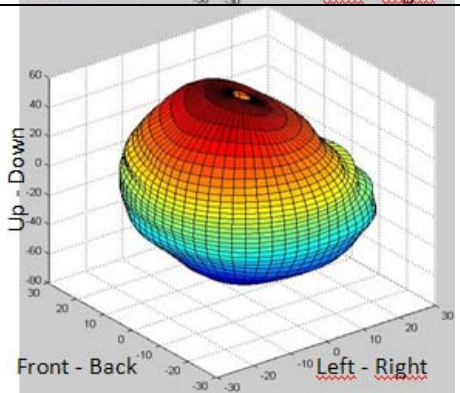
15	256	0.47%	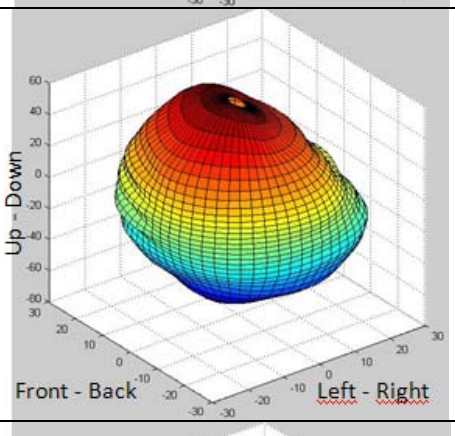
16	289	0.41%	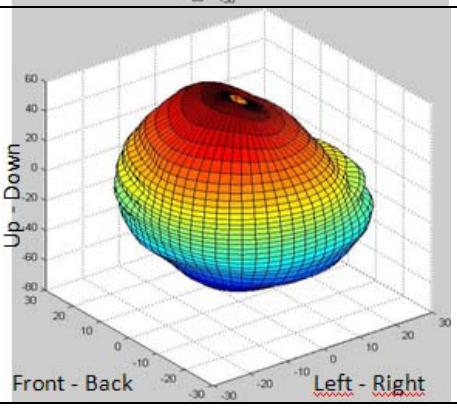

Figure 4.4. Errors and surfaces for different orders of the method

As we can see, the error decreases quickly with the smallest coefficients, but then from order 10 to order 16 we don't get an important improvement, neither with the visual shape or the error. We have to notice that the computer time to create the heart of order 16 can easily be 10 times more than order 9, and the improvement we get it is not even 1%. Another issue we have to take care about is the appearance of strange results in high orders that do not affect the error (as the volume is not affected by small perturbations) but clearly affect the surface of the heart, creating small waves on the shape of the reproduced heart.

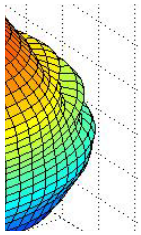

Figure 4.5. Zone of the reproduced heart with irregularities

Because of these previous reasons, we think that a correct choice will be to use order 10, what means using 121 coefficients to reproduce the surface of the heart.

Slicing the spherical harmonic heart

Once our spherical harmonic heart is reconstructed, the next step will be to slice the heart with different planes, different angles and positions, to reconstruct the 2-D projection of the heart in any direction.

The idea is to find the theta and phi that solve both the plane and the heart equations. To work with planes in Spherical Coordinates **[18]**, we will represent each case of the plane equation with spherical coordinates. First of all, we will define the plane as follows:

$$ax + by + cz + d = 0$$

Then, using

$$z = r\cos(\theta)$$

$$y = r\sin(\theta)\sin(\emptyset)$$

$$x = \mathrm{r}\sin(\theta)\cos(\emptyset)$$

We can represent the plane equation in spherical coordinates for all specific case:

a) a,b,c≠0 and d=0

$$r = \cos(\emptyset) + \frac{a}{c}\sin(\theta)\cos(\emptyset) + \frac{b}{c}\sin(\theta)\sin(\emptyset)$$

b) a,b,d≠0 and c=0

$$r = -d\frac{1}{a\sin(\theta)\cos(\emptyset) + b\sin(\theta)\sin(\emptyset)}$$

c) a,b≠0 and c=d=0

$$r = a\sin(\theta)\cos(\emptyset) + b\sin(\theta)\sin(\emptyset)$$

d) General case

$$r = -\frac{d}{c}\frac{1}{\cos(\theta) + \frac{a}{c}\sin(\theta)\cos(\emptyset) + \frac{b}{c}\sin(\theta)\sin(\emptyset)}$$

After having the different equations for all specific cases, we will find the angles that solve the plane and that the difference between the point in the plan and the heart surface is under a certain threshold, and we get the following curves as a result:

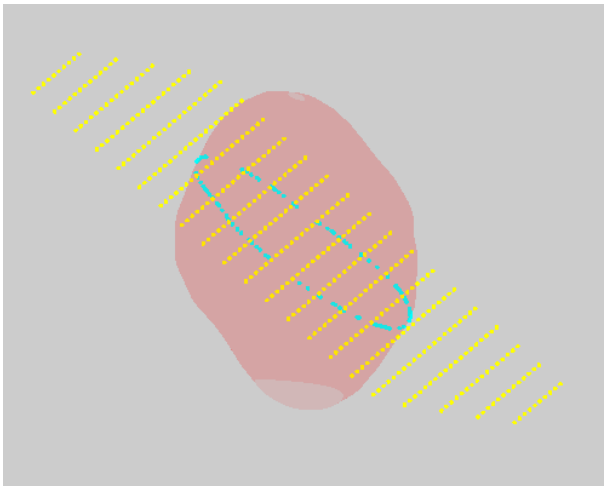

Figure 4.6. Plane that crosses the origin cutting the heart

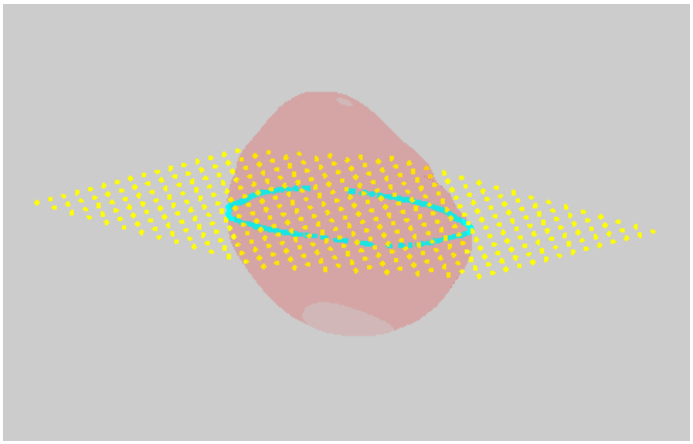

Figure 4.7. Horizontal plane cutting the heart

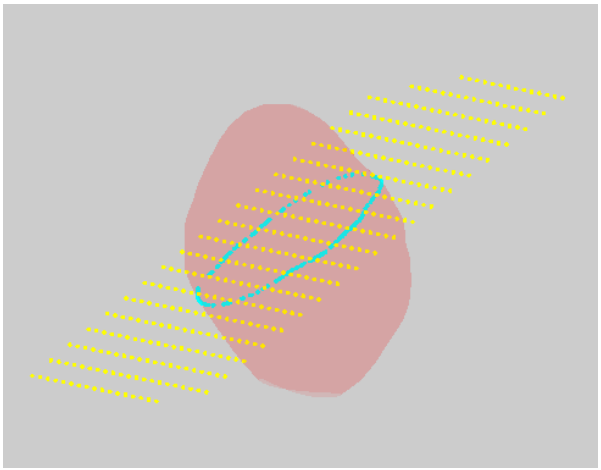

Figure 4.8. Plane that doesn't cross the origin cutting the heart

5. Datasets

The 4D MRI datasets that we are going to work with consist of coronal and saggital images of a healthy human. For each time point (frame) we have one of this volumetric set of images (slice), but we don't have synchronization between the instants of different slices. Our aim is to connect the slices with the same respiratory phase and to segment the heart in each of these respiratory instants. Doing this we could reconstruct a 4D model of the heart motion due to the respiration.

The MRI datasets acquisition parameters are the following:

	View	Modality	Intra slice resolution	Inter slice resolution	Temporal resolution
DATA1	Coronal Dataset	MRI	1.5mm x 1.5mm	7.2mm	1 frame per second
	Saggital Dataset	MRI	1.5mm x 1.5mm	7.2mm	1 frame per second
DATA2	Saggital Dataset	MRI	2mm x 2mm	8mm	3 frames per second
	Navigator	Marker			

Figure 5.1. Datasets information

DATA1

The image acquisition is done by acquiring multiple successive slices for different time point at the same cardiac cycle moment. The acquisition is triggered by an ECG signal and several cycles of the breathing must be acquired. The imaging is done at the same beating phase to avoid beating motion.

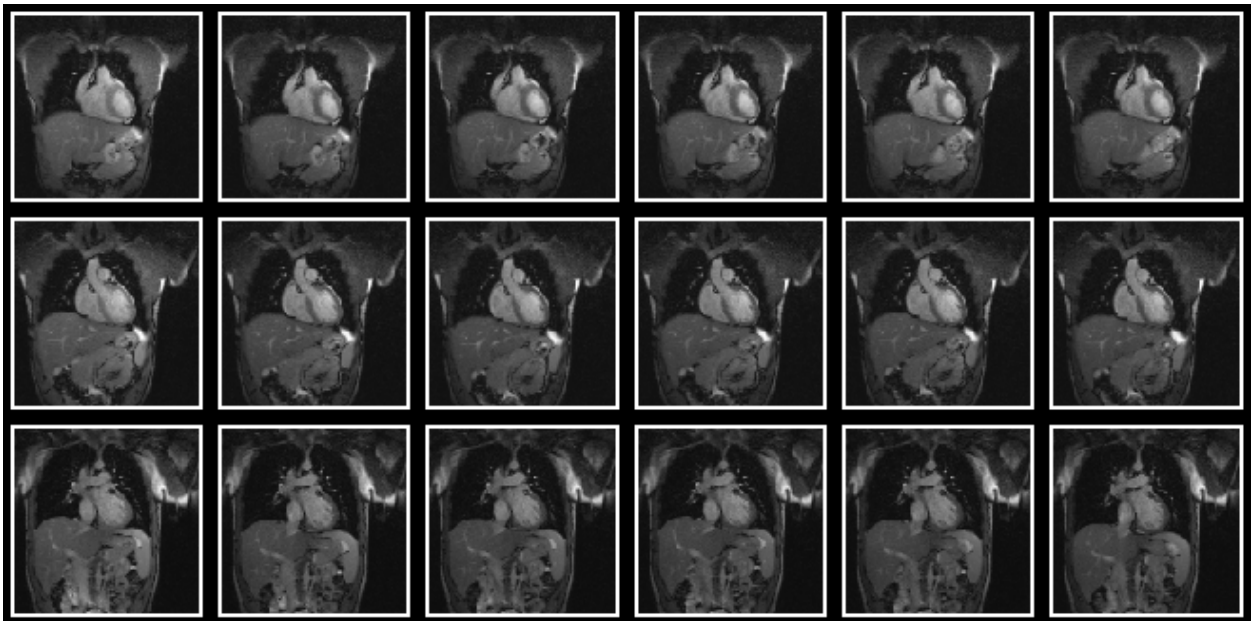

Figure 5.2. Subset of the Coronal Dataset, showing different slices and frames

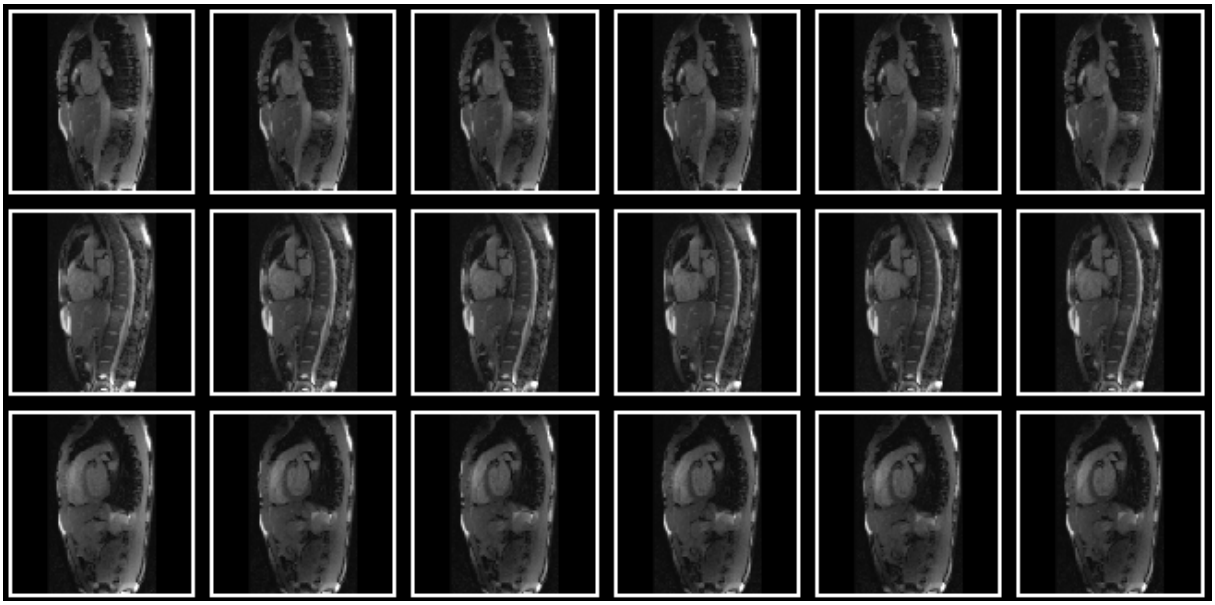

Figure 5.3. Subset of the Saggital Dataset, showing different slices and frames

The datasets have a different global coordinate system, meaning that a point in a dataset and the same point in the orthogonal one are not in the same global position. This problem will be solved during the project.

DATA2

DATA 2 has some differences with DATA 1. First of all, the temporal resolution is bigger, having 3 frames per second instead of only 1. This can be done because DATA 2 is not ECG gated, so it is possible to acquire more than 1 image per cardiac cycle.

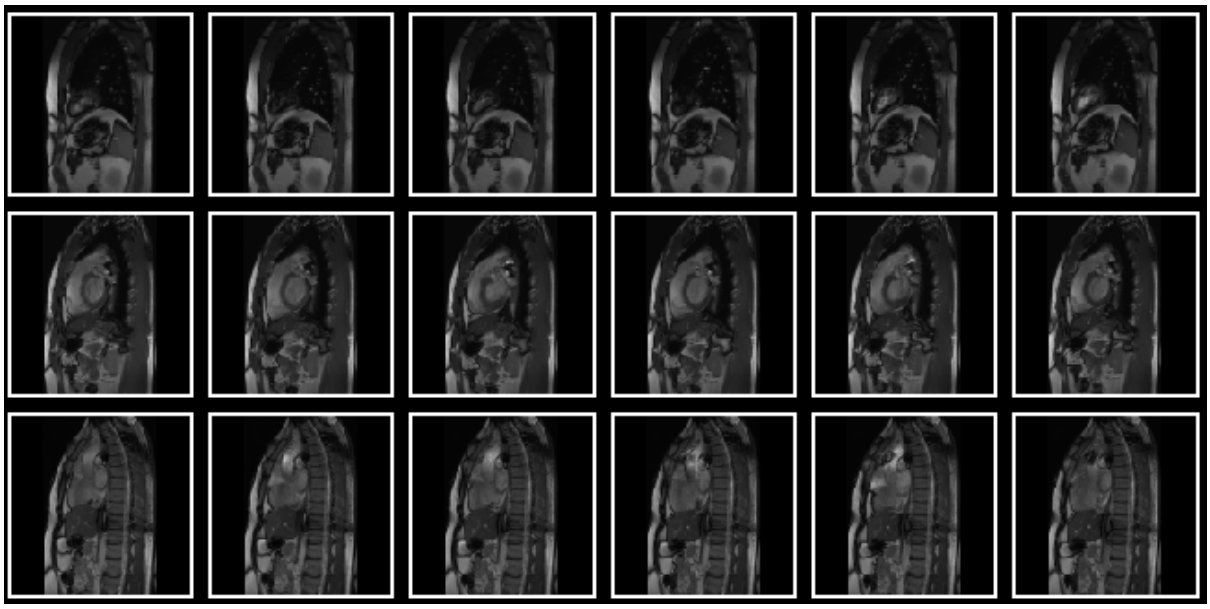

Figure 5.4. Subset of DATA2, showing different slices and frames

The other difference between DATA2 and DATA1 is that DATA2 also includes a navigator that shows the respiratory phase of each frame, what will make our work easier.

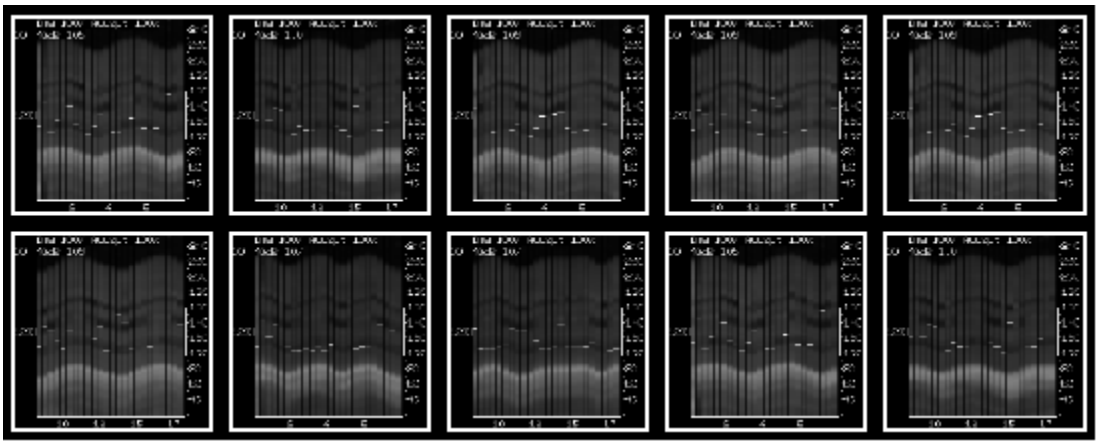

Figure 5.5. Navigator included in DATA2, showing the respiratory phase of each frame

CHAPTER 2: Working with ECG gated data (DATA1)

1. Introduction

In Chapter 2 we will study the ECG-gated data, and we will try to extract from it the respiratory motion of the heart and all the information we can about the respiratory cycle.

As we explained in Chapter 1, DATA1 is ECG-gated data, which means we don't observe the beating of the heart **[19]**. This will make our work easier in terms of finding the heart at every instant, and tracking its movement, but as the heart rate of our volunteer is more or less 60 beats per second, we will have around 1 image per second. This poor temporal resolution will affect our results and as we will show, make it impossible to extract the respiratory motion from the data we are using.

2. Estimation of the respiratory cycle

When trying to estimate the respiratory motion of the heart, we can easily find a big problem with our data. We don't want to see the beating movement of the heart, so the images of the human chest are taken all in the same cardiac instant and thus we don't see the heart beating, we only see the movement due to the respiration. If the heart beat of a healthy human being is around 70 beats per minute, it means that we have around 70 images per minute (actually we have 60, one per second, see DATA1). Now if we think about the period of a respiratory cycle of a healthy human being, which is around 12–20 breaths per minute, it has a period of 3 to 5 seconds. With both rates, we easily see that we will have in our data only 3, 4 or 5 images per cycle, which makes for a very poor sampling.

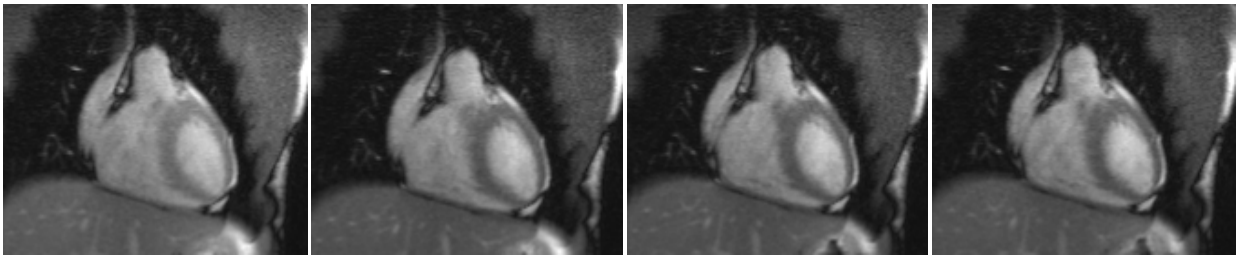

Figure 2.1. Images of a respiratory cycle

The next problem will find is the tiny movement that the heart does during the respiration. According to **[20]**, and after some experimental observation, we have seen that the movement in the coronal slices (bottom-top cuts) is less than 11mm, 7 pixels, and in the sagittal slices (left-right cuts) it is even smaller, around 2mm (2 or 3 pixels). This fact will increase the difficulty of quantifying the respiratory phase with individual values. We will use splines instead and that will give us more precision.

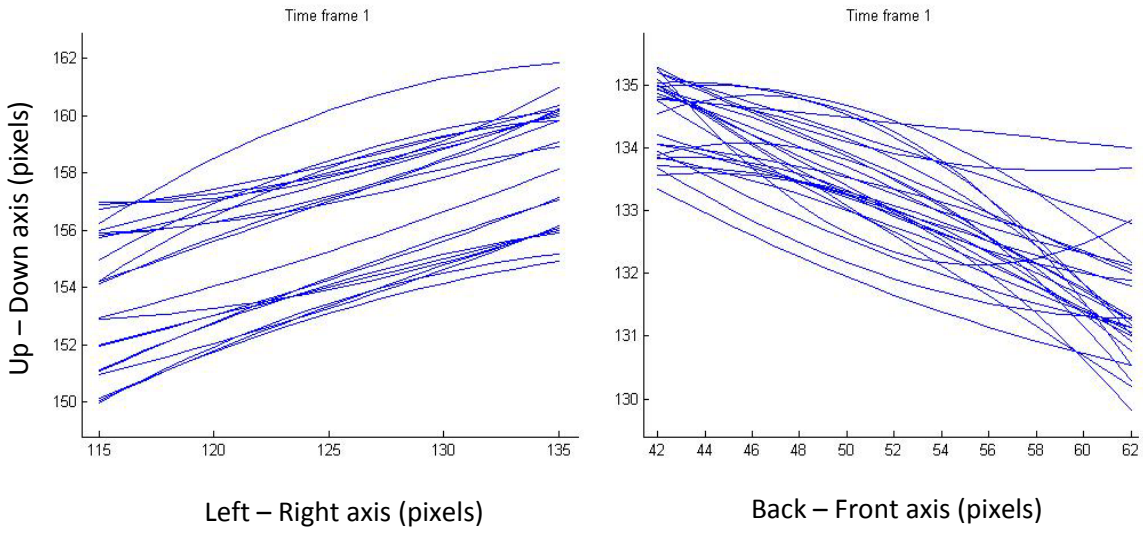

Figure 2.2. Curves than represent the movement of the liver during 30 seconds in the coronal slices (left) and the saggital slices (right). We can see that the variations of pixels from one slice to another are very tiny.

We have to take care of all these problems if we want to represent the heart movement with accuracy and reliability.

The image set we are using has no synchronization (in time or in respiratory phase) between slices, so for us it is impossible to know where we are in terms of respiratory phase when we see an image. Because of this, we are forced to develop some algorithms that extract information from the datasets we have to explain the respiratory frequency, the regularity of the volunteer's breathing, and also order the frames to show the heart motion due to respiration.

Body wall approximation

The first approximation of the heart position (or the respiratory phase) we thought to use was the body wall position. We use the body wall position in each frame to know the relative phase position of the frame inside all the slice frames. After preprocessing the data and selecting some points in the left side of the body, our algorithm finds the body wall of each frame, using the binarized image as an indicator of when the body wall appears. Another point we have to be careful about is the direction of motion in the images. Comparing the position of the body wall of the actual frame with the next one, we have to divide the frames into categories of "increasing" and "decreasing". Then this method finds the best curve that represents the body wall, and put the slices in order, creating a simulation of the respiratory cycle for each slice. This information allows us to find the phase of each frame inside all the full circle of 30 frames of any slice, and we can put all the images in the corresponding order.

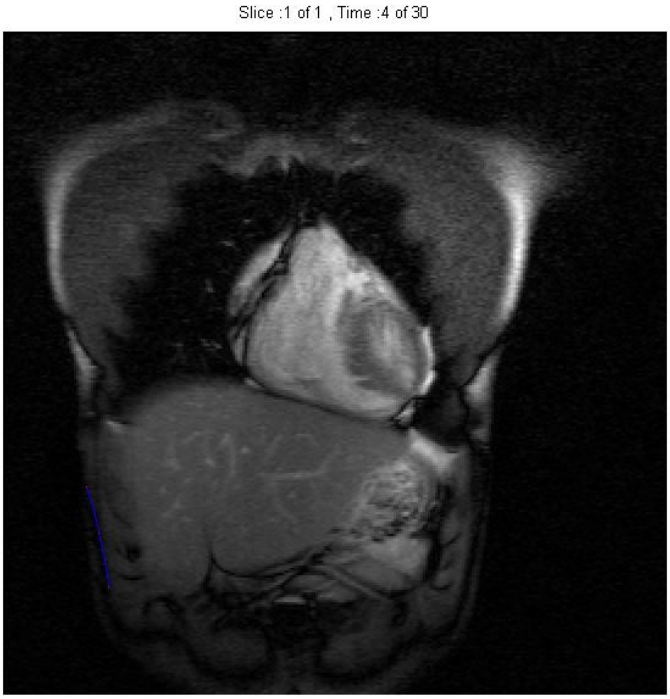

Figure 2.3. Curve (in blue) that represents the body wall of this frame

With this information we also can find a lot of results about the respiratory cycle of the data set we are using, like the frequency, or whether it is constant.

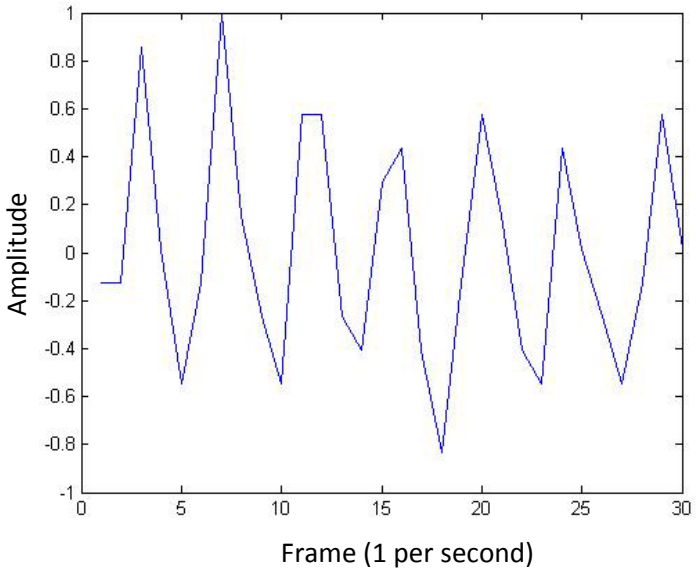

Figure 2.4. Values of the body wall detection algorithm, fitted between -1 (less movement of the body wall) to 1 (biggest movement)

Liver approximation

The second approximation we use to find the phase of the different frames in the dataset is the liver movement **[21]**. The liver is a huge organ, which makes it easier to track its movement. Again after selecting some points next to the liver surface, we use the liver position to estimate the frame phase inside the respiratory cycle. The method is very similar to the previous one; the only difference is the organ we are using to detect the points. The liver has some advantages when trying to estimate the respiratory cycle, such as the size, or the smoothness and bigger magnitude of movement **[22]**, but also has some drawbacks. The most important one is that the liver doesn't appear in all the slices, but only in the ones in the middle of the heart, not in the ones in the external region; which means that we only can extract information from around 70% of the slices. In the slices where the liver curve is not clear at all, or it is not possible to detect, we have to use other curves or other techniques.

With this algorithm we get the following measurements of a respiratory cycle:

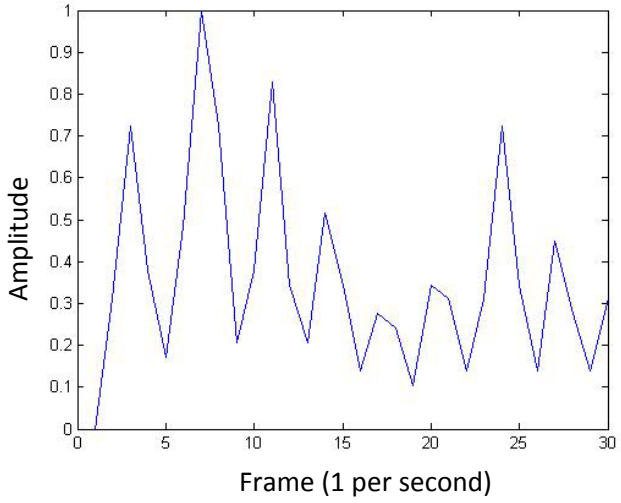

Figure 2.5. Values of the liver algorithm acquisition, where we can see again that the volunteer is breathing without any pattern

The advantages of using the liver instead of the body wall are:

- The liver has a longer movement than the body wall, which means more resolution and bigger range of values.
- The liver is easier to find in the MRIs, because is bigger, clearer and it's easier to find a bunch of points to initiate the algorithm.

As we said before, the drawbacks are that the liver changes at every slice: not only its position, but also its shape and orientation.

MUSIC algorithm to find the respiratory frequency

Once we have captured the liver or body wall movement, the first thing we are interested in is to know the predominant frequency of the respiratory cycle. As our data is very under-sampled, and we have only a few samples of every cycle, we will try to use the MUSIC algorithm to find the best sinusoid that fits our data.

MUSIC algorithm

The MUltiple SIgnal Classification (MUSIC) frequency estimation method was proposed as an improvement on the Pisarenko harmonic decomposition **[23]** by Bienvenu and Kopp **[24]**, and Schmidt **[25]**.

The MUSIC algorithm is an eigen-based subspace decomposition method for estimation of the frequencies of complex sinusoids observed in additive white noise. Consider a noisy signal vector $\boldsymbol{y}$ composed of **P** real sinusoids, modeled as:

$$\boldsymbol{y} = \boldsymbol{S}\boldsymbol{a} + \boldsymbol{n}$$

Where

$$\boldsymbol{a} = [X_1\ X_2\ \ \ldots\ \ X_p]$$

$$\boldsymbol{S} = [s_1\ s_2\ \ \ldots\ \ s_p]$$

$$s_k = [1\ \ e^{j2\pi f_k}\ \ \ldots\ \ e^{j2\pi(N-1)f_k}\ \ ]^T$$

N is the number of samples, f_k is the frequency of the k-th complex sinusoid, X_k is the complex amplitude of k-th sinusoid and $\boldsymbol{n}$ is a zero mean Gaussian white noise vector with variance σ_n^2.

The autocorrelation matrix of the noisy signal y can be written as

$$R_{yy} = E[yy^h] = \ R_{xx} + \ R_{nn} = SAS^H + \ \sigma_n^2$$

Where E denotes the expectation, H denotes Hermitian transpose and $A = E[aa^H]$ is the diagonal matrix. In addition, $R_{xx} = SAS^H$ and $R_{nn} = \sigma_n^2\boldsymbol{I}$ are the autocorrelation matrices of the signal and noise processed as

$$R_{xx} = \sum_{k=1}^{N} \lambda_k\ v_k\ v_k^H$$

$$R_{nn} = \ \sigma_n^2 \sum_{k=1}^{N} v_k\ v_k^H$$

Where λ_k and $\boldsymbol{v}_k$ are the eigenvalues and eigenvectors of the matrix R_{yy}. All the eigenvalues are real numbers and satisfy

$$\mu_1 \geq \mu_2 \geq \cdots \geq \mu_p > \mu_{p+1} = \cdots = \mu_n = \sigma_n^2$$

Then, the MUSIC spectrum (Pseudospectrum) is defined as

$$P_{xx}^{MUSIC} = \frac{1}{\sum_{k=P+1}^{N} |s^H(f)\boldsymbol{v}_k|^2} = \frac{1}{s^H(f)\,\boldsymbol{V}\boldsymbol{V}^H s(f)}$$

Where $s(f) = [1 \;\; e^{j2\pi f} \;\; \ldots \;\; e^{j2\pi(N-1)f}]^T$ is the complex sinusoidal vector and $V = [v_{p+1} \ldots v_N]$ is the matrix of eigenvectors of the noise subspace.

MUSIC algorithm applied to our data

In our particular case, we will use the MUSIC algorithm to, given all the liver or body wall movements, find the best sinusoid that represents all the data. First of all, we have to create a matrix with all of our data. We have 19 slices, and 3 points per slice. As we have 30 frames for all the slices, we have

$$D = \begin{bmatrix} mov(1,1) & \ldots & mov(1,M) \\ \ldots & \ldots & \ldots \\ mov(N,1) & \ldots & mov(N,M) \end{bmatrix}$$

Where the columns are the 3 points of all the 19 slices (N=57) and the rows are the 30 samples of each point of each slice.

Using the SVD decomposition, we can express D as

$$D = USV^H$$

Where U is an NxN matrix, V is an MxM matrix, and S is an NxM diagonal matrix. The columns of V form a set of orthonormal “input” basis vector directions for D, while the columns of U form a set of orthonormal “output” basis vector directions. The matrix S contains the singular values, which can be thought of as scalar “gain controls” by which each corresponding input is multiplied to give a corresponding output.

Once we have the decomposition of our data matrix, we visualize the singular values, to try to separate the data associated with noise and the real data. We expected to see a big difference with the singular values (which would mean that we have a clear dominant frequency in our data, and the rest is noise), but as the data we are using is based on natural breathing, irregular and without any control, what we get is the following:

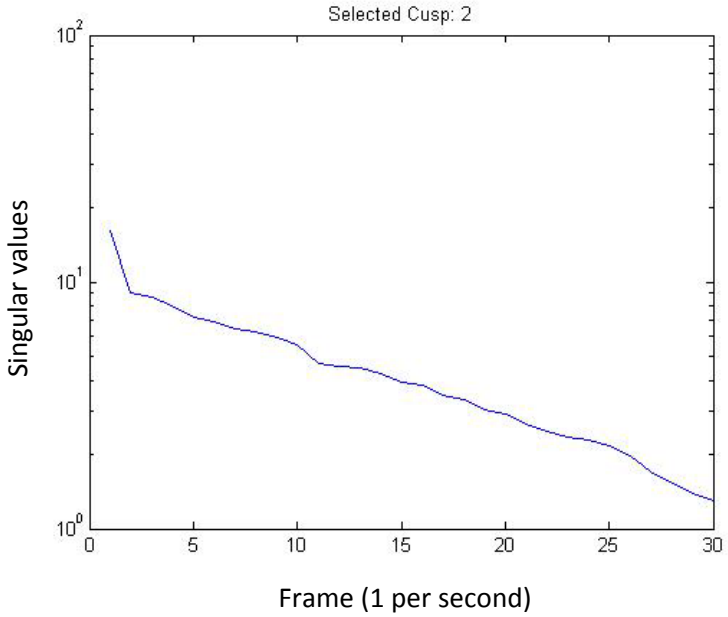

Figure 2.6. Singular values for the 30 samples

We can appreciate that we don't find a huge difference between the singular values, but we can see a big jump between the first and the second. We can interpret this as the jump between frequencies that appears more in our data, but we have observed that there are other frequencies with relevant importance in the liver or body wall movements.

Once we select this jump as a border between real data and noise, we calculate all the noise pseudospectrums for several different frequencies,

$$P_k^{MUSIC} = \frac{1}{s^H(f_k)\,\boldsymbol{V_{noise}}\boldsymbol{V_{noise}}^H s(f_k)}$$

where S is the sinusoids vector for a given k frequency, and $\mathrm{V}_{\mathrm{noise}}$ are the V columns associated to the noise.

After calculating all the pseudospectrums, the index *k* with the maximum value will give us the minimum noise, so the frequency that better represents all of the 57 (= 19 slices *3 points/slice) movements of our liver or body wall.

For the concrete case of the liver movement during 30 seconds and 3 points per slice, we have the following results, where we can see different input data (liver movement during 30 seconds for a given slice) compared with the best sinusoid we can find:

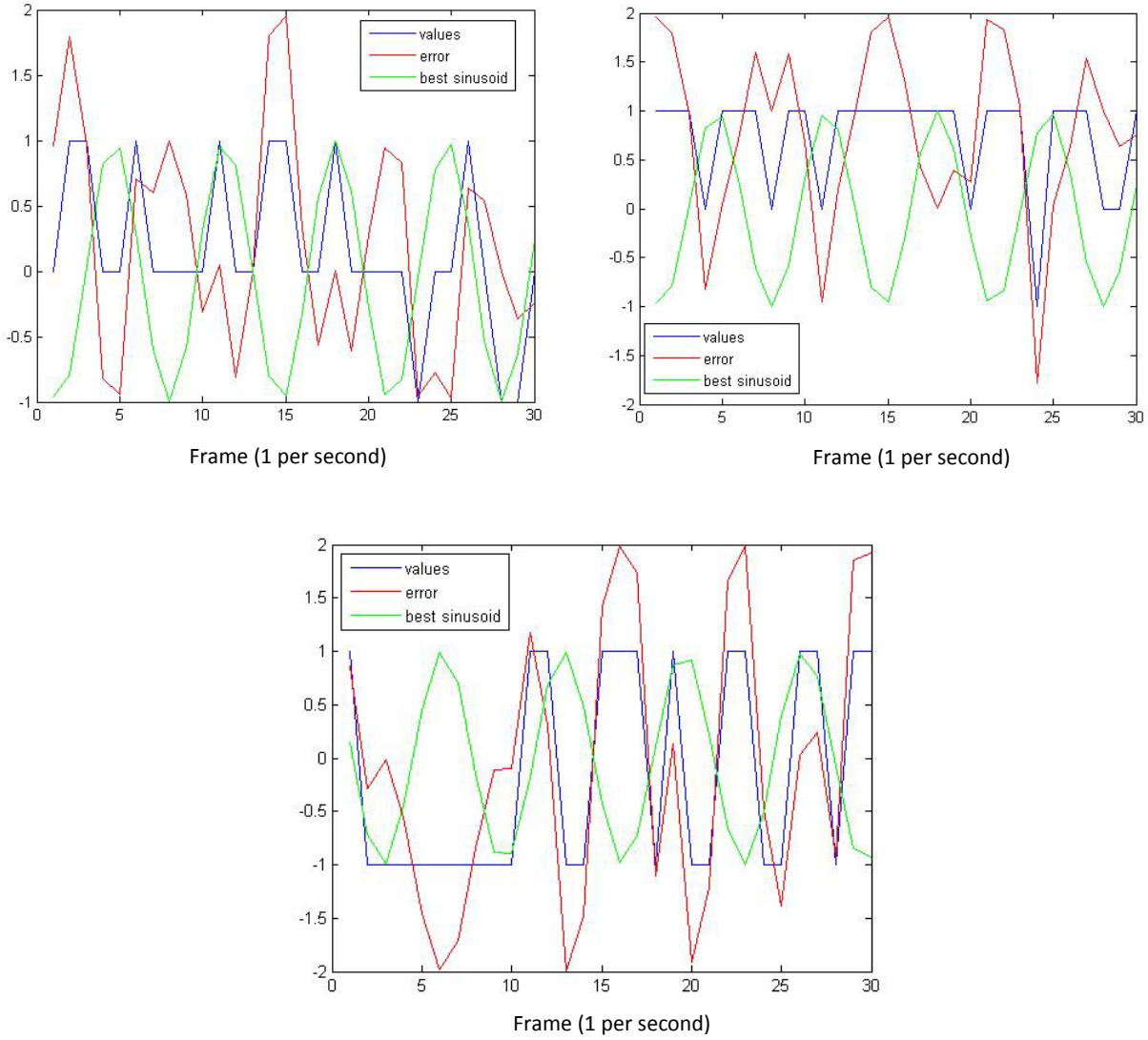

Figure 2.7. Different input data compared with the best sinusoid

In the previous figure we can clearly see the problem with the data we are using: the breathing of the volunteer is not constant, which makes it impossible to find a frequency that can fit all of the data. In addition, the undersampling causes some data to not have all of the range of values, which increases the error significantly.

3. Results of these first methods

Working with DATA1 means having only between 4 and 6 samples per respiratory cycle, which means also having less than 3 samples per half respiratory cycle. With this poor sampling it is impossible to reproduce an entire respiratory cycle, even more because of the fact that DATA1 has only 30 frames per slice (30 seconds of data). In the next section we will try to use the 3D information (using the 2 datasets at the same time to try to reproduce the cycle), because using only one (that is what we have been doing until this point), it is not enough to reach good results.

After studying the data and the possibilities it has, we strongly think that it is possible to achieve good results with ECG-gated data if one has more samples. That is to say that even with the strong drawback of having only 6 samples per cycle (in fact 3 samples per half a cycle, because we are working with half a cycle all the time), if we had 60 or 70 images instead of 30, we would have a lot of samples and we could reconstruct the respiratory cycle with much more precision.

The biggest problem is that we don't have samples in all the respiratory instants, what is translated in big jumps in our data (see figure 2.7). If we had more temporal resolution, this problem would be solved, but with ECG-gated data this is not possible. The other option is having the same temporal resolution having much more samples. More samples means more cycles, so when we extract the information from the cycles, we will have more cycle samples to compare and with which to work.

The next step will be to use the 3D nature of our data, which is to say: use both the saggital and coronal datasets to try to solve the problems caused by undersampling and poor resolution we have, hoping that using the liver surface in the 2 directions will allow us to know the respiratory phase of each slice.

4. Adding 3D information to the liver acquisition

The drawback of these first approximations is that the result we get after applying the algorithms is only local, we are using the frames of each slice separately, creating a different ordering in every slice. In other words, we are only creating a correct simulation of the breathing cycle at any slice separately, not for the complete heart data. The next step will be to mix the information of the different slices, using this information to connect them and create a better representation of the respiratory cycle.

With this next step we want to use the information of both datasets to know the relation between one slice and the next. As the datasets are related and both have redundant information, we want to use all the frames of one slice to determine the positions of the other slices respect to this one and be able to connect the slices between them.

As the following figure shows, both datasets have points in common around the heart, fact that we want to use for our purpose.

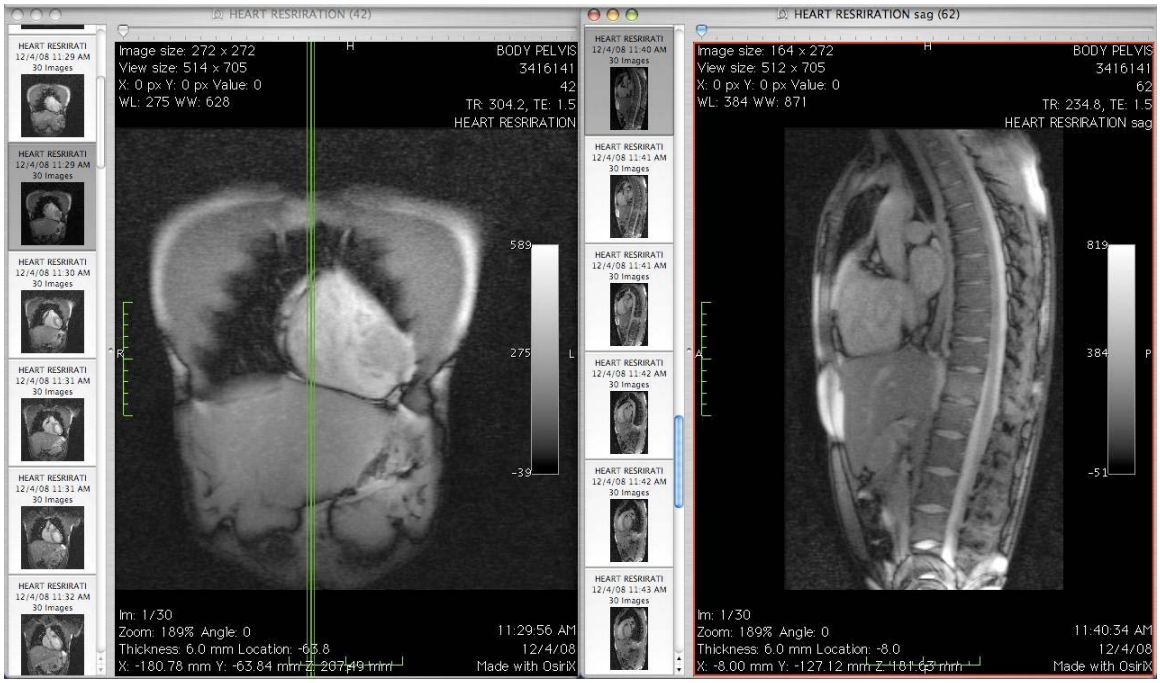

Figure 4.1. In the right, saggital slice. In the left, coronal slice. The green line shows the position of the saggital slice respect to the coronal slice

The idea is, selecting one slice in the saggital dataset, find in the coronal dataset the liver points that correspond to the next slices in the saggital dataset, so we can find out the correspondence between different slices in one phase instant. If this is done for all the 30 frames, we should know the values of the different slices in the saggital set and we could put them in order according to the respiratory phase.

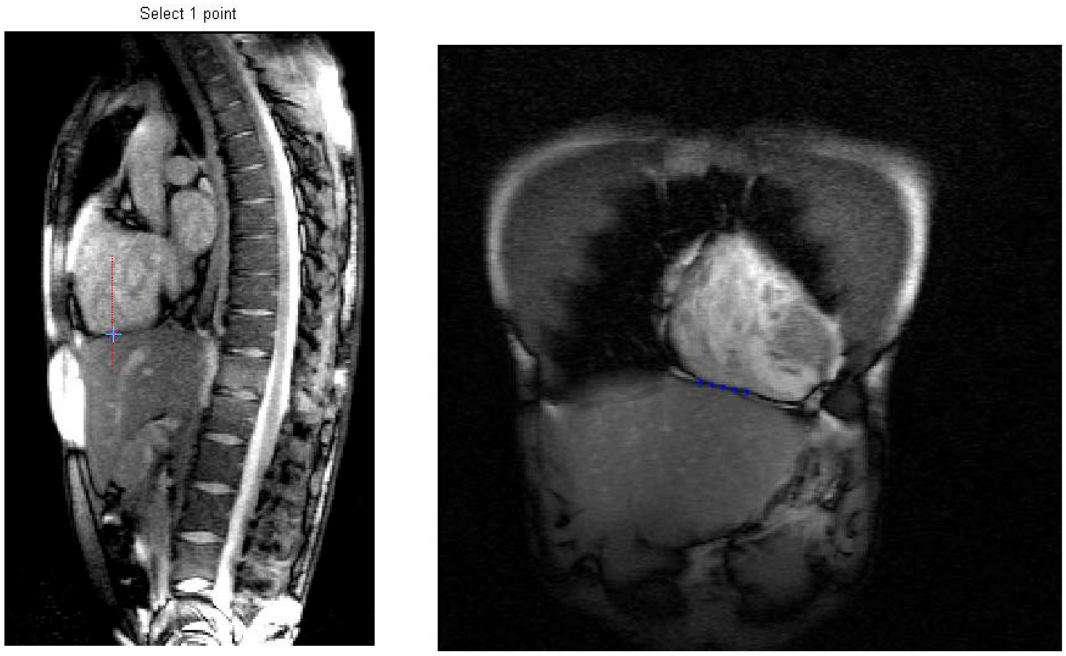

Figure 4.2. Left image, our algorithm allowing us to select the point between the liver and the heart. Right image, our algorithm detecting the liver positions for the next slices

The first problem we find with this method is that the datasets have different global coordinates, what makes it impossible to associate one point in one dataset with the same point in the other dataset. So first of all we have to convert all the points to the same basis.

The algorithm we will use to solve this problem finds for any point in the saggital dataset the range of values in the coronal dataset, and converts the saggital range to the coronal range. After this we can compare both datasets and apply our 4-D detection algorithm to find the heart movement.

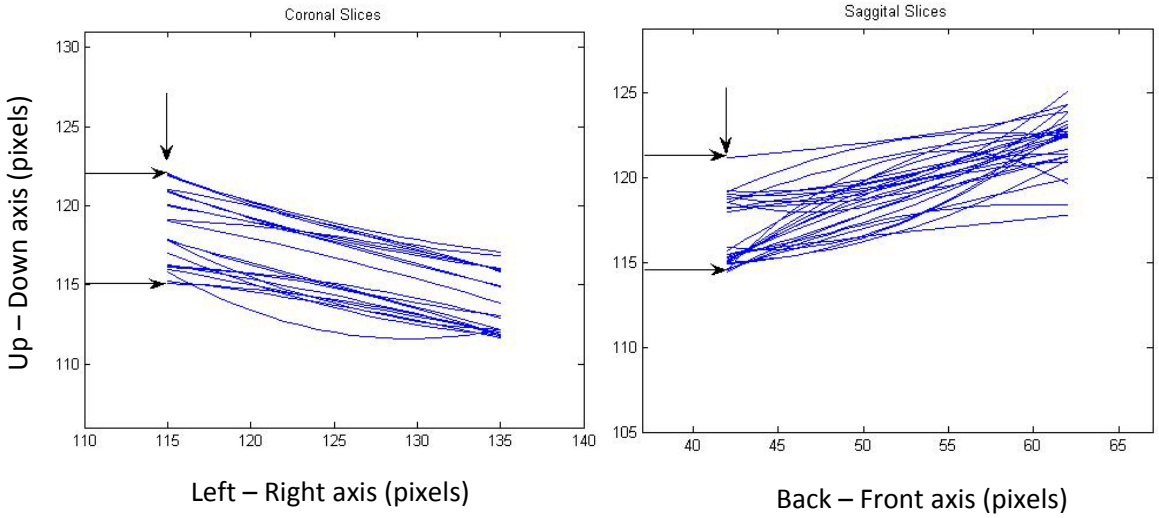

Figure 4.3. Same point in the coronal slices (left) and saggital slices (right) after converting all the liver points

The first step is to select the point in common where both slices (coronal and saggital) have the liver surface. Once we have selected this point (that will tell us the phase on the first slice), the algorithm finds the points that the following slices should have in this phase instant.

Using the information of both saggital and coronal slices we can represent the liver surface, and as we know that the heart movement has a high correlation with the liver motion, we can represent the respiratory phase in terms of liver position for each frame of each slice.

The problem with this method is again the poor sampling and the fact that we only have 30 frames per slice. These 2 drawbacks make clear that when we have a point in one direction, and we try to find the same point in the other view, the probability of finding a frame with this value is very low. So in fact what we are doing is a 0 order interpolation (finding the closest frame of the 30 frames we have in one direction) for each frame in the other direction.

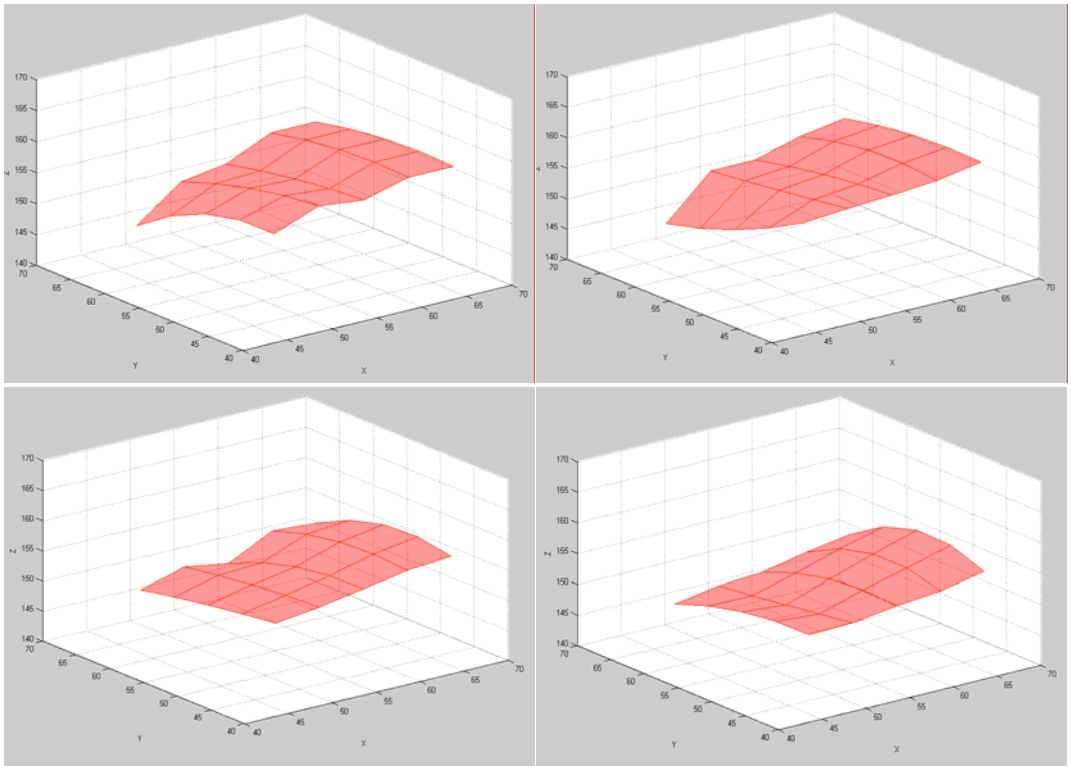

Figure 4.4. Liver reproduced using 3D information

5. Final conclusions about working with DATA1

After trying different solutions to extract the respiratory motion from DATA1, the conclusions that can be extracted from our work are:

I. Having the MRIs gated to the beating helps when finding the heart boundary, the liver boundary or the body wall. On the other hand, the ECG gating makes it impossible to have more than 1 frame per second.
II. More time resolution is needed, with only 1fps we can't reproduce the respiratory cycle.
III. More frames are needed. Even with 1fps, we need more than 30 frames per slice to extract the respiratory motion.
IV. Information about the phase of each frame would be useful, helping to avoid finding the respiratory phase for all the frames.

CHAPTER 3: Working with ungated data (DATA2)

1. Introduction

The third chapter of this Thesis will study the advantages and disadvantages of using ungated data to extract the respiratory motion of the heart. As we have previously discussed, ungated data will add some difficulties to heart tracking and detection due to the beating motion. On the other hand, the fact that the data extraction is not gated by the heart beat will give us a greater sampling rate, which will be very useful for extracting the respiratory phase of each frame.

This chapter will explain the methods we have used to extract the heart shape from DATA2, the respiratory phase of each frame, and finally how the respiratory motion is reproduced. As will be explained later in the chapter, the respiratory cycle is divided, and each frame is associated with the nearest division point. Then two methods are used to reproduce the respiratory motion: the first one creates one independent heart at every operating point, and uses these hearts to reproduce the movement. Then a second method is presented, where we assume that the heart is a rigid body and we model the motion using the centroids of each “operating point” heart.

Both methods are compared and their drawbacks and advantages are exposed, concluding with some examples and images of the final results.

2. Proposed method

According to the previous conclusions and suggestions, the new data we are going to use in this chapter will be DATA2, an ungated data, which has 3fps, and 50 frames per slice. We have also a navigator with the respiratory phase of each frame. For more information, see DATA2.

To achieve our goal, we will use and compare 2 different techniques. The first one will divide the respiratory cycle in M instants, reproduce the heart at every instant, and use the M reproduced hearts to represent the real motion. The second one will use the results of the first one to create an averaged heart of all the hearts, and using the centroid positions of the M hearts and its rotations, represent the respiratory motion of the heart. The steps to achieve our goal are the following:

i. Extract the respiratory phase of each frame
ii. Find the heart boundary for all the frames and all the slices
iii. Divide the respiratory cycle in M operating points
iv. For every operating point, select all the frames with a similar respiratory phase and average them, creating a 2-D heart boundary for all the slices and all the operating points
v. Finish of the first technique. Check if the M hearts are a good representation of the respiratory motion
vi. Find the centroid of each heart
vii. Create the averaged heart of all the 10 hearts using Spherical Harmonics
viii. Reproduce respiratory motion using the averaged heart and the centroids
ix. Add rotation to the motion
x. Check the results with this second technique

In the first stage, our method will segment the heart boundary, to be able to reconstruct the heart at every operating point. With this information we want to reconstruct the respiratory motion, knowing how the heart will look like at every respiratory phase. The next step (the second technique), will be to model the translation and the rotation of the motion, and use spherical harmonics to represent the moving heart.

3. First technique

Extracting the respiratory phase

The first step in our method is to extract the respiratory phase for every frame. In previous chapters we used the body wall and the liver surface to try to extract this information, but with the new data we have, which includes the navigator, we will extract the respiratory phase information more easily.

The navigator consists of a DICOM file with some information that is not relevant for our study, and also contains 24 columns with a different grey value, representing the respiratory phase of 24 frames. As we have 50 frames per slice, there are 3 images per slice, with the last one having 22 repeated values, and only 2 new.

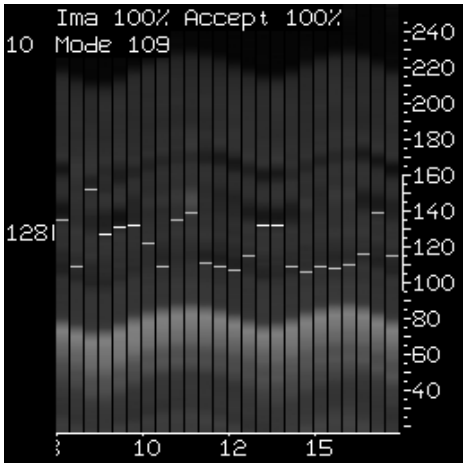

Figure 3.1. Image representing the respiratory phases of 24 frames

The first step will be finding the values of the brightest wave (the one centered on 80). After choosing a maximum and minimum y value for the wave (see figure 7.2), we will calculate all the first derivatives, and the first one to exceed a certain threshold will be the point we associate to the respiratory phase.

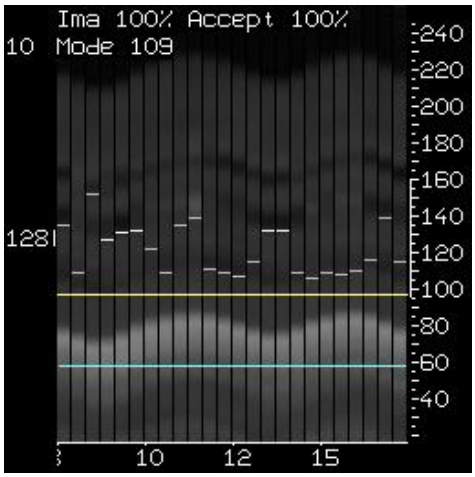

Figure 3.2. Maximum and minimum y values selected

Looking at the image, one can appreciate that there are a lot of waves that represent the respiratory cycle, but the one that is better for us is the one between the 2 horizontal lines (minimum and maximum values that we select). Then, after calculating all the first derivatives only inside this range, we can find easily the points with a higher jump, shown in red on figure 7.3.

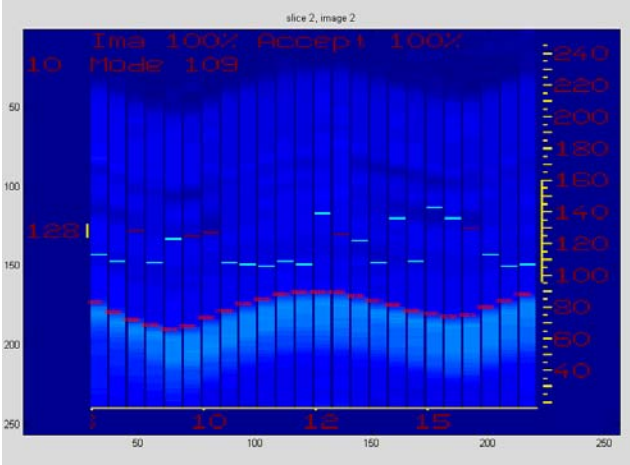

Figure 3.3. In red, the points found with the algorithm

Finally, we use only one point per column, and we process all the navigator images (3 images per slices, having 18 slices). After processing the images, we get all the respiratory phases of all the frames, and we can reproduce some respiratory cycles:

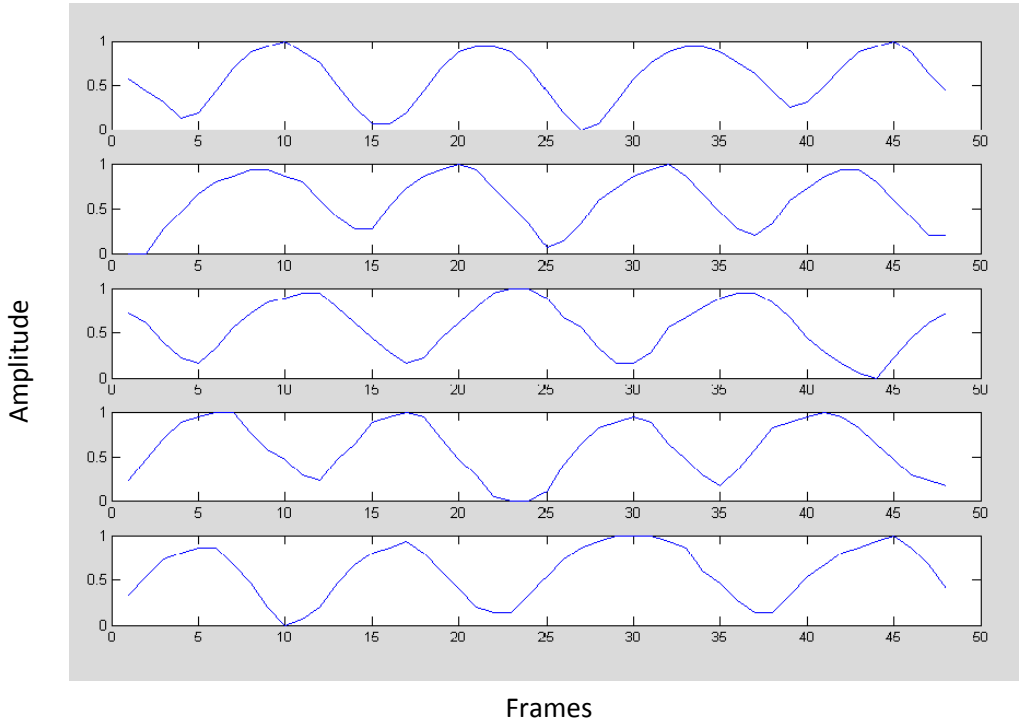

Figure 3.4. Reproduced respiratory cycle for different slices

Finding the heart boundaries

The second step of our method is finding the heart boundaries for all the frames and all the slices. As the heart moves up and down and from the left to the right due to the respiration, and also has the beating movement, the algorithm we are going to use will be based on manually selecting the center of the heart and from this point, we will find the first point under a certain threshold (which we also manually select).

The first problem we find using this method is the existence of black holes in some frames due to the beating, which makes our algorithm find points near the center. Obviously those points are not boundaries, so we do not want to consider them. Another problem is the fact that in some slices there is no boundary between the heart and other organs like the liver, and because of that the algorithm does not find any points or finds a point too far from the center that can't be a boundary.

To solve both problems we create a minimum and a maximum radius for all the slices. Knowing that the heart is smaller in the external slices and bigger in the middle ones, we choose a minimum radius that will prevent the algorithm from thinking that the holes are boundaries, and we choose a maximum radius that will do the same thing but with non-boundaries areas. Figure 3.5 contains different radiuses for different slices.

Figure 3.5. Maximum (white) and minimum (red) radiuses for different heart slices

After selecting the centers and creating the radiuses, the algorithm has to find the boundaries of the heart. Every point inside the two circles will be taken, but if the algorithm finds the point outside this region, it won't take that point into consideration. The basic idea is that we prefer not to find a point in one direction than finding a "false" point. As we will interpolate in polar coordinates the points, if we have a region without points, it will be closed with a continuous radius. Figures 3.6 and 3.7 show the points we find for different slices.

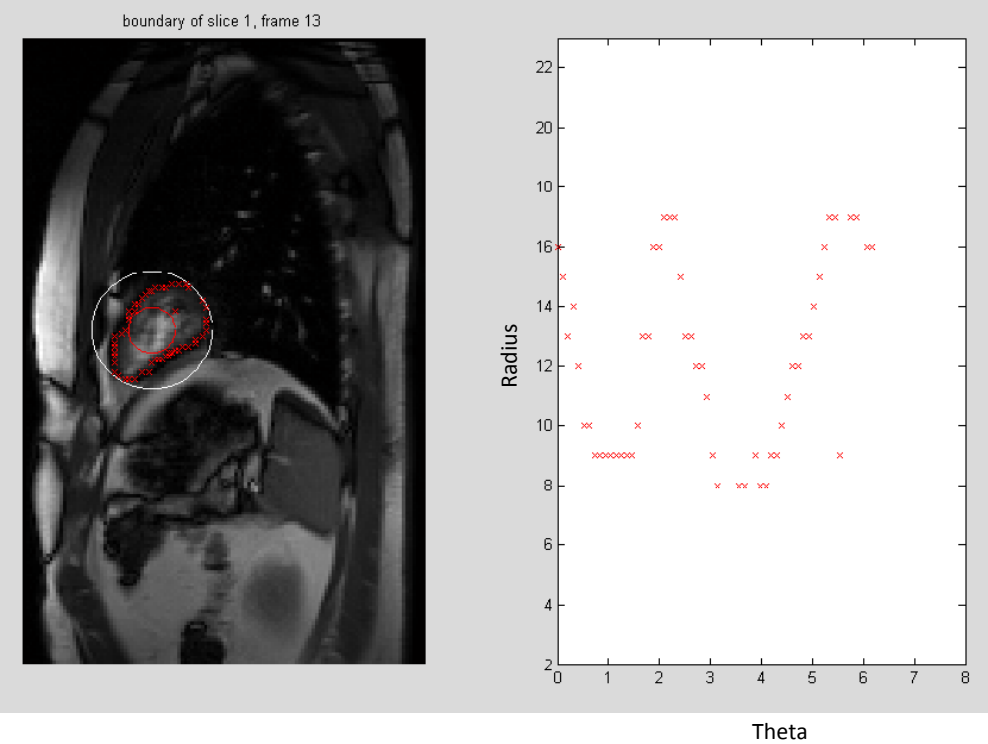

Figure 3.6. Points found in the first slice and 13th frame. In the left, on the real MRI. In the right, represented in polar coordinates

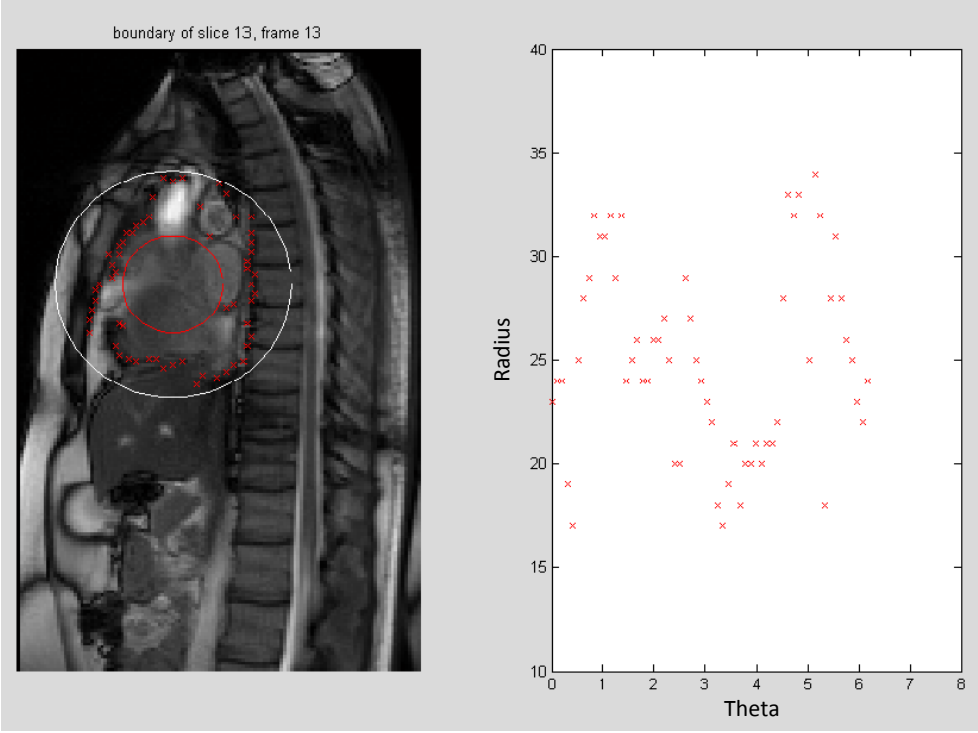

Figure 3.7. Points found in the 13th slice and 13th frame. In the left, on the real MRI. In the right, represented in polar coordinates

Once the points are detected, the next step is closing the gaps between them. To perform this action, we tried both spline and linear interpolation **[26]**, having better results with the second option. What we do, always in polar coordinates, is a linear interpolation between the points. Where there are no points, the linear interpolation will create a straight line that converted to Cartesian coordinate will be a curve of constant radius.

Moreover, the spline interpolation will use cubic splines to fill the gaps, and this will create cubic curves in polar coordinates, so radius variations in Cartesian coordinates.

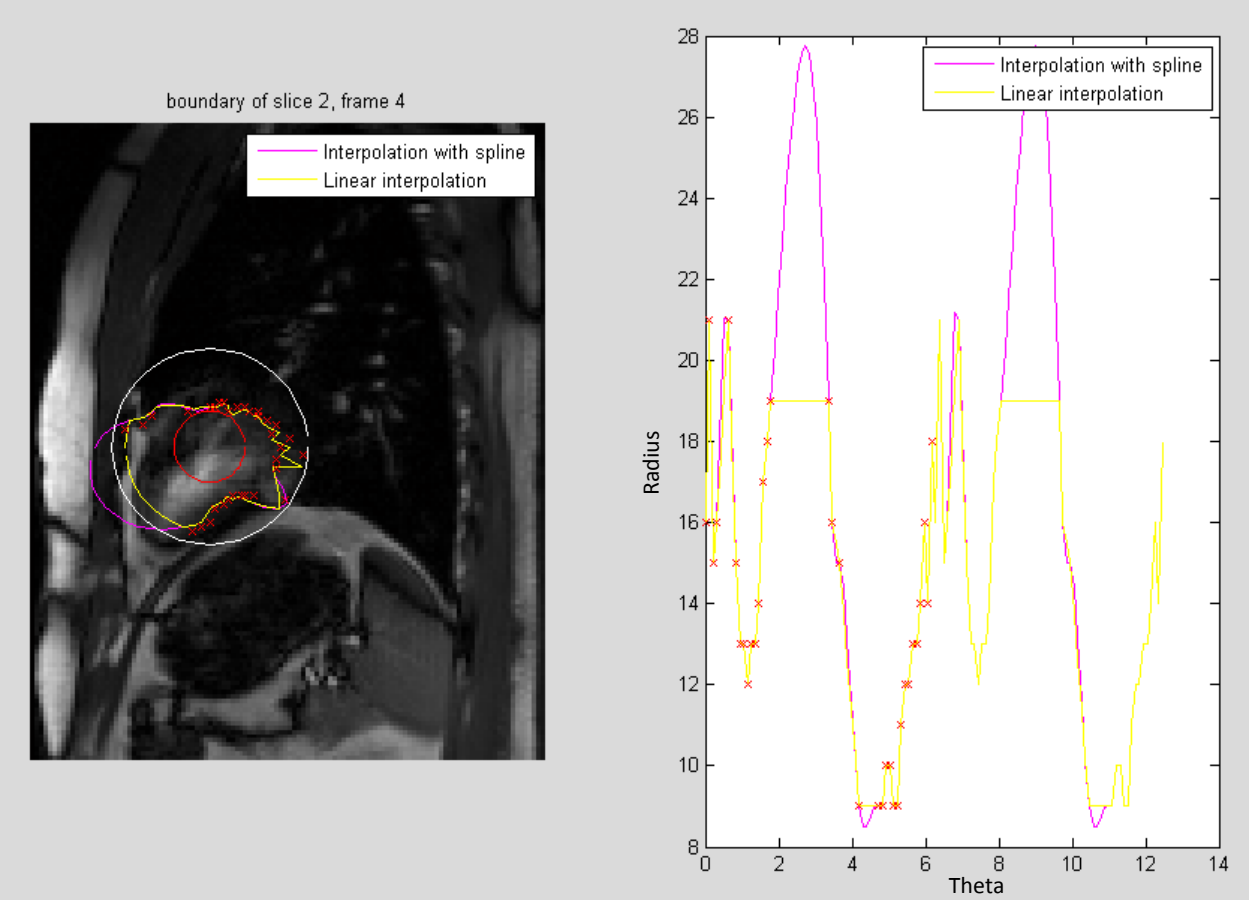

Figure 3.8. Linear (yellow) and spline (pink) interpolations of the found points (red). Polar coordinates in the right side of the figure, Cartesian coordinates in the left side.

The last step to find the boundaries will be to filter the interpolated curves. As we can see in Figure 3.8, we have a lot of unwanted jumps between the points, and this can easily be solved using an IIR filter **[27]**, with W samples that averages the curve.

$$c(n) = \frac{1}{W}\sum_{i=0}^{W-1} c(n-i)$$

We use a window of 4 samples (W=4), and we average the curve as can be seen in Figure 3.9.

Figure 3.9. Filtered curve that represent the heart 2-D boundary

Now we have a boundary of the 2-D heart for all the frames (50) of all the slices (16) of the heart. So that is to say that if the data had been synchronized, we would have 50 3-D hearts. As for one frame of one slice we can't find the same phase in the next slice, we don't have 50 complete hearts, but 50 samples of the respiratory motion for all the slices where the heart appears.

As we have the respiratory phase of all the frames, we can try to associate frames of different slices using their phase, and recreate the heart at some positions. This will reproduce the heart at different respiratory phases.

Divide the respiratory cycle in M operating points

Once we have all the heart boundaries, we want to represent the respiratory cycle as a variable from 0 to 1, and we will divide this new variable in M operating points, where we will reconstruct the heart.

As we have 50 samples per slice, we suggest use M=10, so we will have on average 5 samples per operating point. The more divisions we make, the better phase resolution we will have, so if the data had more samples, M should be higher.

For all the slices we divide the respiratory phase as figure 3.10 shows, and all the frames with a value close to the division value are taken. “Close” will depend of M, in our case, all the frames 0.05 above and below the division value are taken into consideration to reproduce the heart at every operating point.

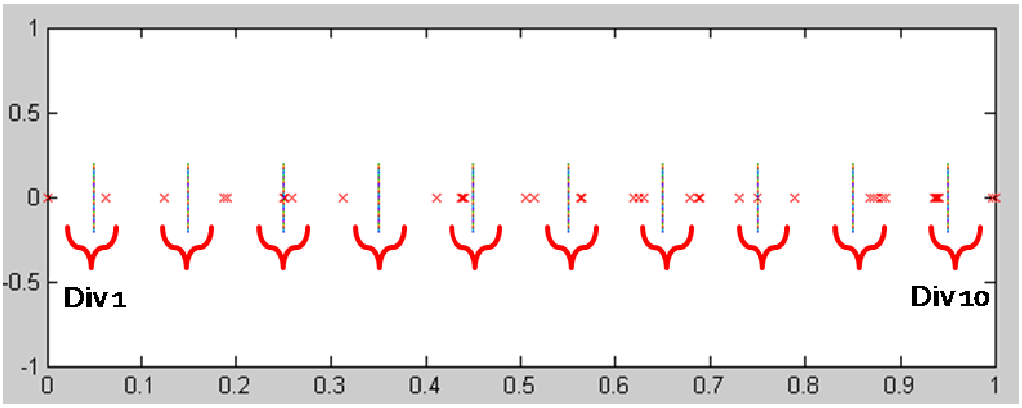

Figure 3.10. Respiratory cycle divided in 10 phase instants

Now we have per every division some samples of the heart. In some divisions we will probably have more than 6 or 7 samples of the 2-D boundary, but in other divisions we will have only 1 or 2. We will use this boundaries to reproduce the heart at every operating point, creating one heart per every division, that have to represent the respiratory position of the heart at a particular respiratory phase.

Reproducing a 3-D heart for every respiratory phase division

The principal idea of averaging all the frames with a similar respiratory phase is eliminate the beating movement of the heart. Our assumption is that if we have enough samples, and equally spaced in the beating cycle, averaging the curves will eliminate the movement of the heart due to the beating, and will keep the respiratory motion. As we said before, the more samples we had, the better this assumption would work.

For our particular case of having 10 divisions, 10 hearts will be created averaging the boundaries. Some results can be seen in the following figures:

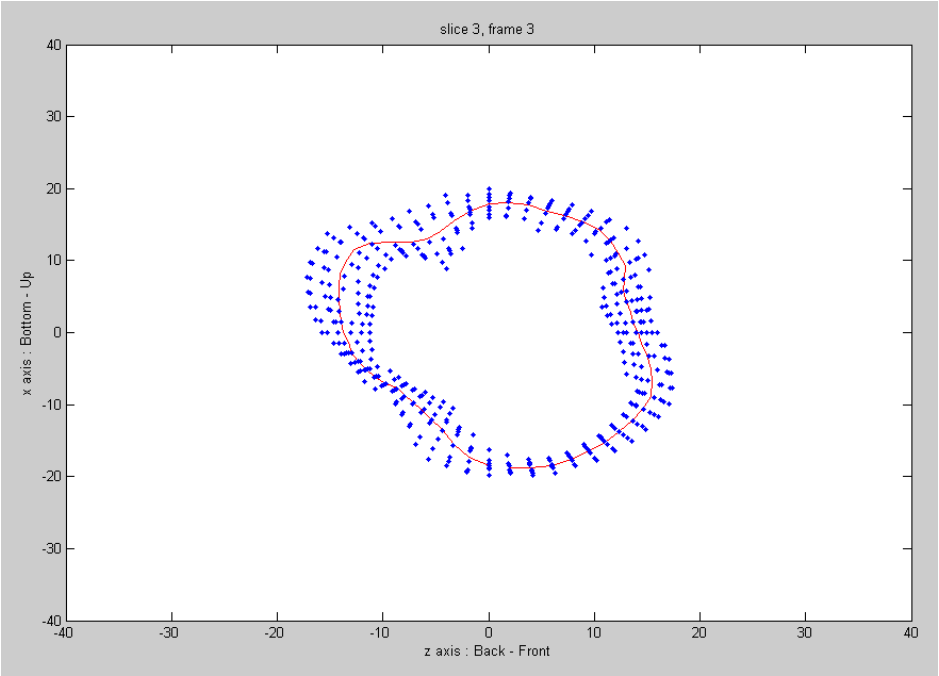

Figure 3.11. Blue points representing the original curves, and red curve representing the averaged curve of the heart for the 3rd slice of the 3rd phase division

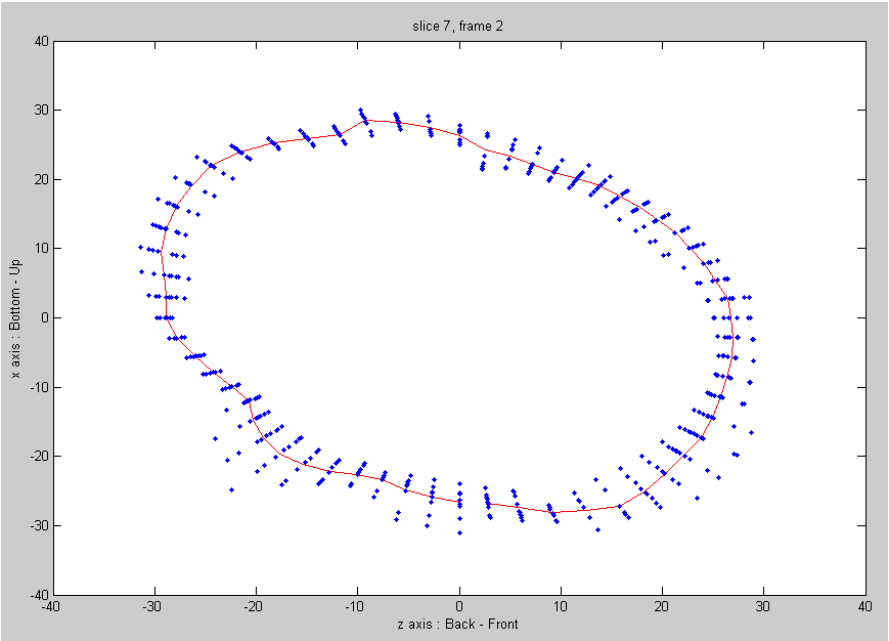

Figure 3.12. Averaged 2-D heart for the 7th slice of the 2nd phase division

And we can also check how the 3-D averaged heart looks like at every phase division, as figure 3.13 shows:

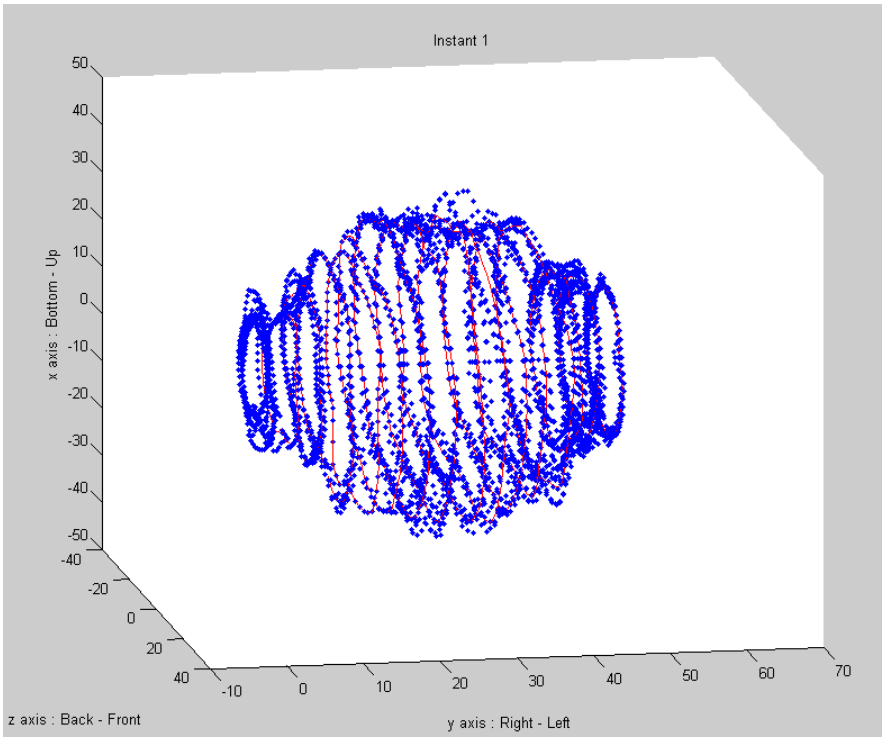

Figure 3.13. Reproduced 3-D heart for the first phase division. Blue points showing the real boundaries used to average, and red curves represent the averaged heart

Results of the first technique

With this first technique we can reproduce the respiratory motion of the heart using M 3-D hearts.

First, we want to check if the M hearts are able to reproduce a real respiratory cycle, in order to say if they represent correctly the movement of the MRIs during an entire respiratory cycle.

To reproduce the respiratory cycle with DATA2, M images are taken for all the slices. Each image represents one of the previous M divisions, so we expect the hearts to be able to represent the MRIs. We can appreciate in the following figures different heart slices following a reproduced respiratory cycle for every slice.

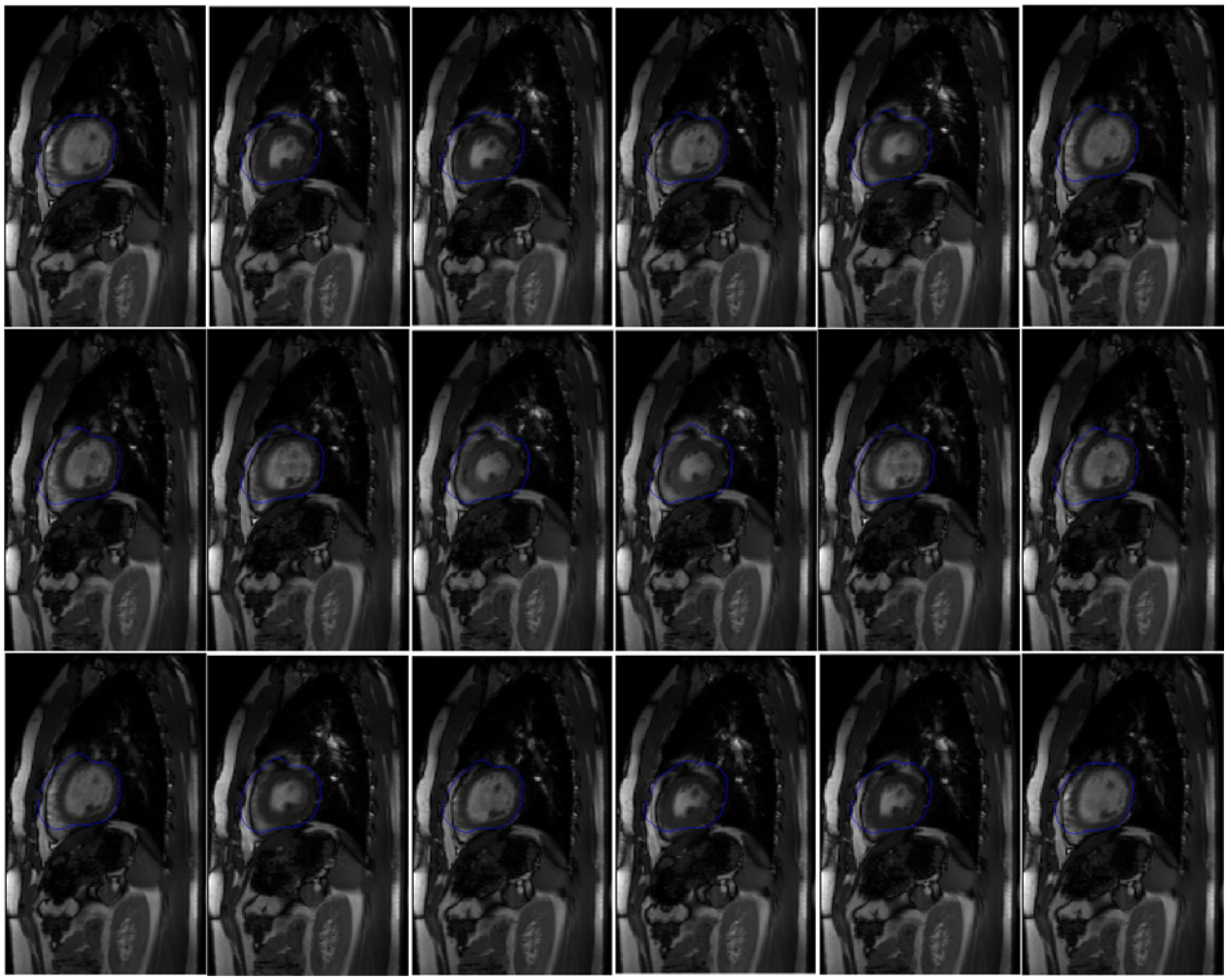

Figure 3.14. Heart following a reproduced respiratory cycle for the 5th slice

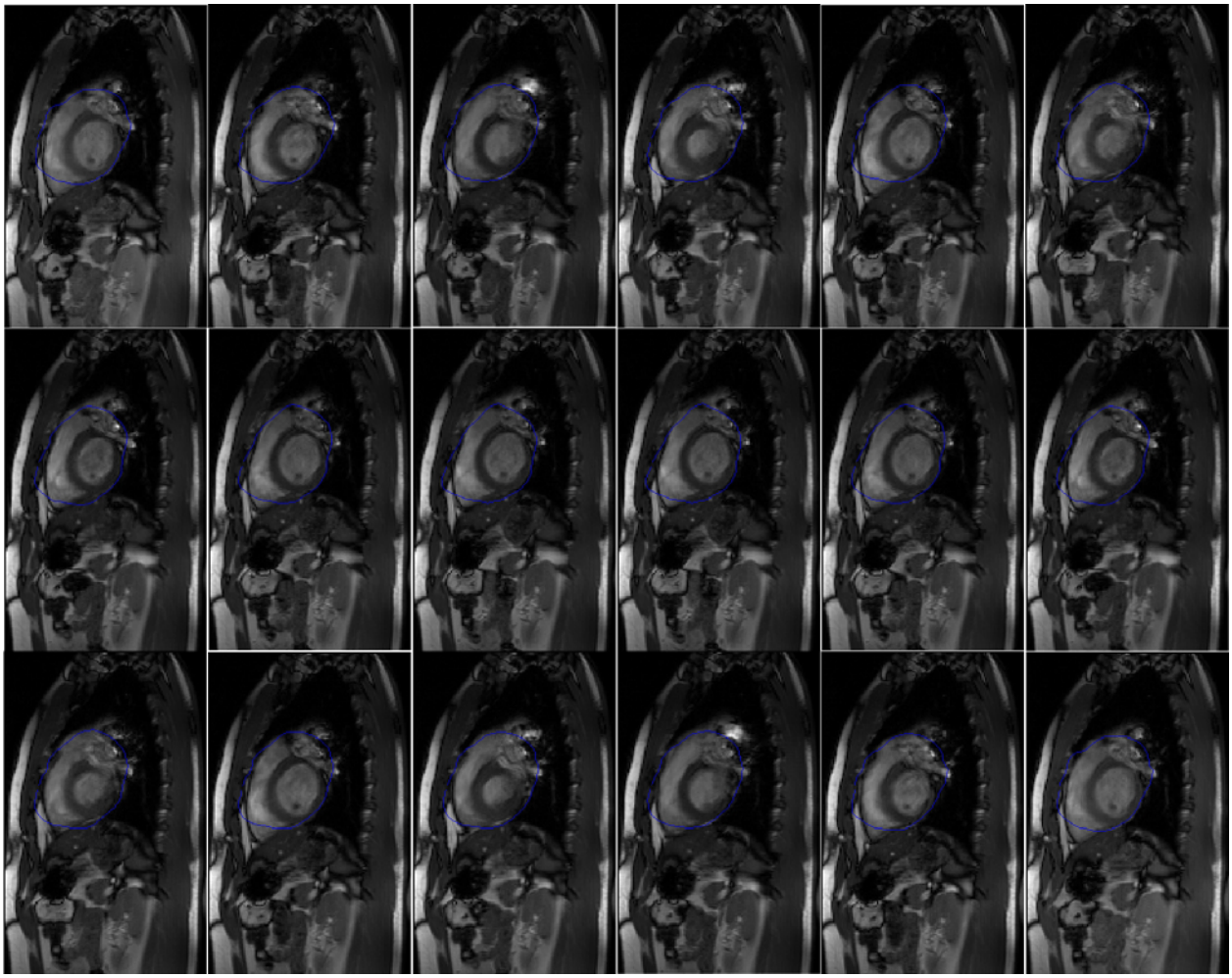

Figure 3.15. Heart following a reproduced respiratory cycle for the 7th slice

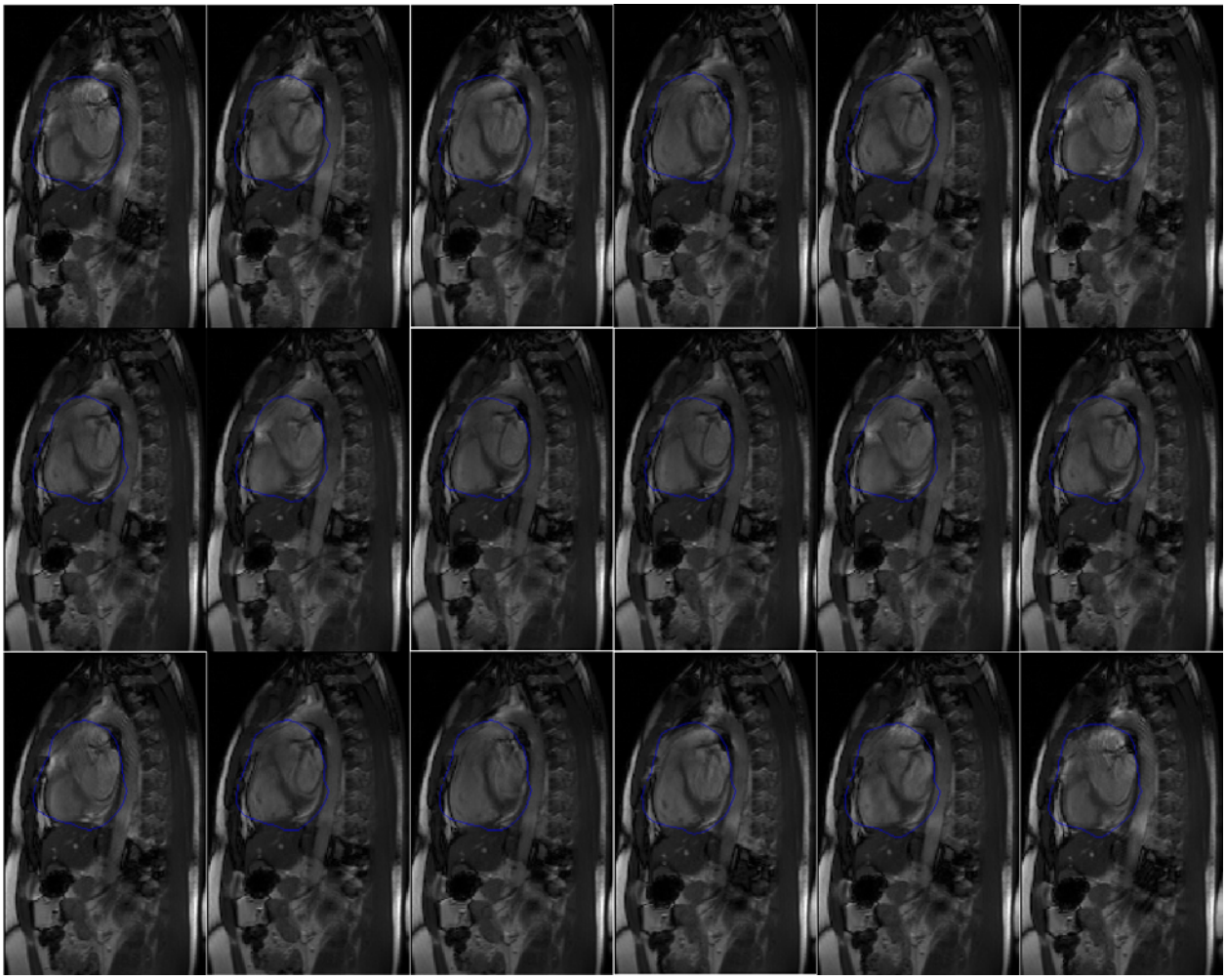

Figure 3.16. Heart following a reproduced respiratory cycle for the 10th slice

Once we have checked that our first technique can represent a respiratory cycle with accuracy, we want to know if we can follow the real data. Before, we were selecting for each heart the slice that best represented the respiratory phase, creating a respiratory cycle. What we want to do know is the opposite; this is for each real MRI, find the heart that has a closest respiratory phase, and assume that we have enough divisions to consider that the selected heart will be a good representation of the MRI.

In the following figures we can see how the M hearts follow the real data for some frames and some slices:

Figure 3.17. M hearts following the real data for some frames of the 7th slice

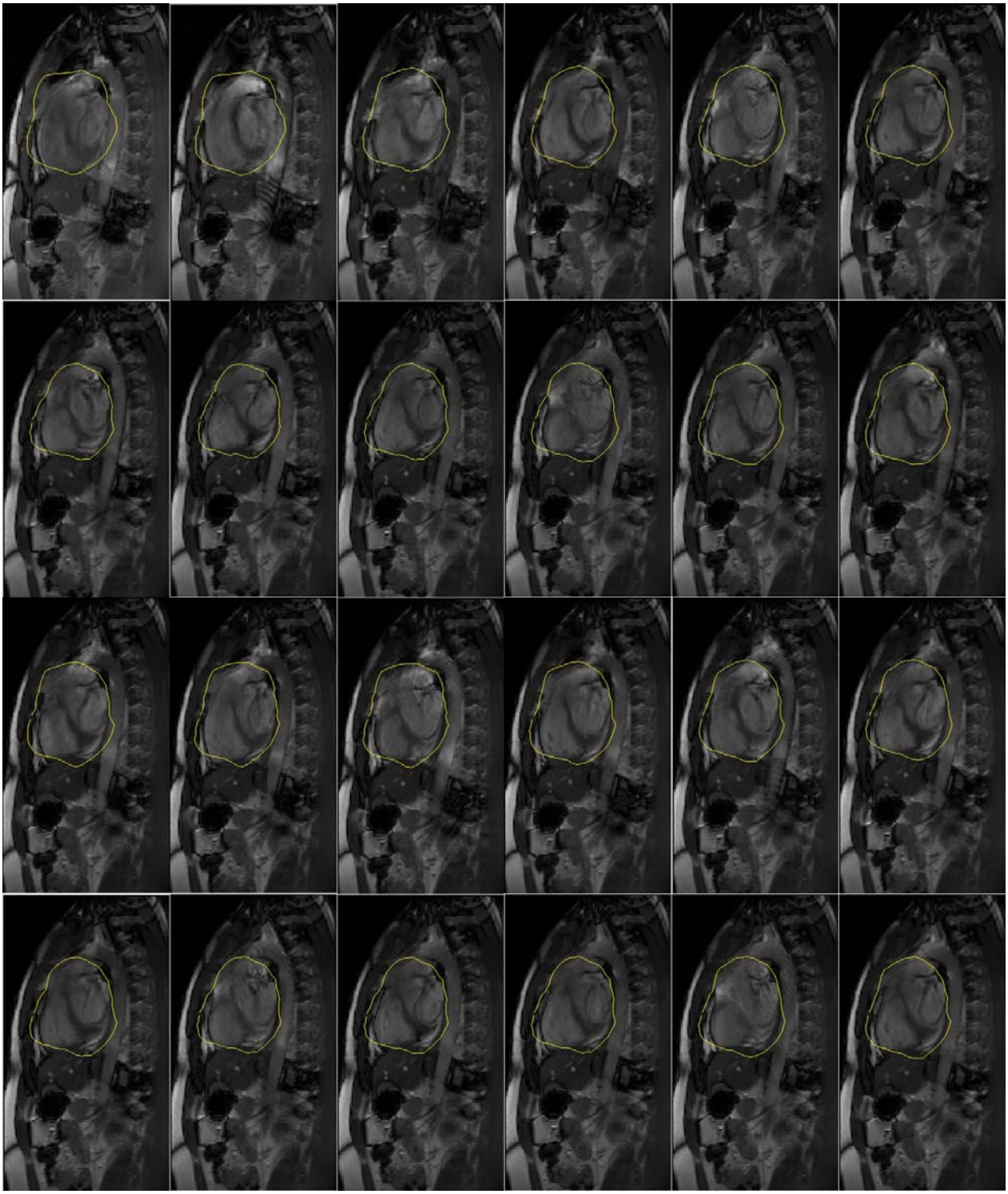

Figure 3.18. M hearts following the real data for some frames of the10th slice

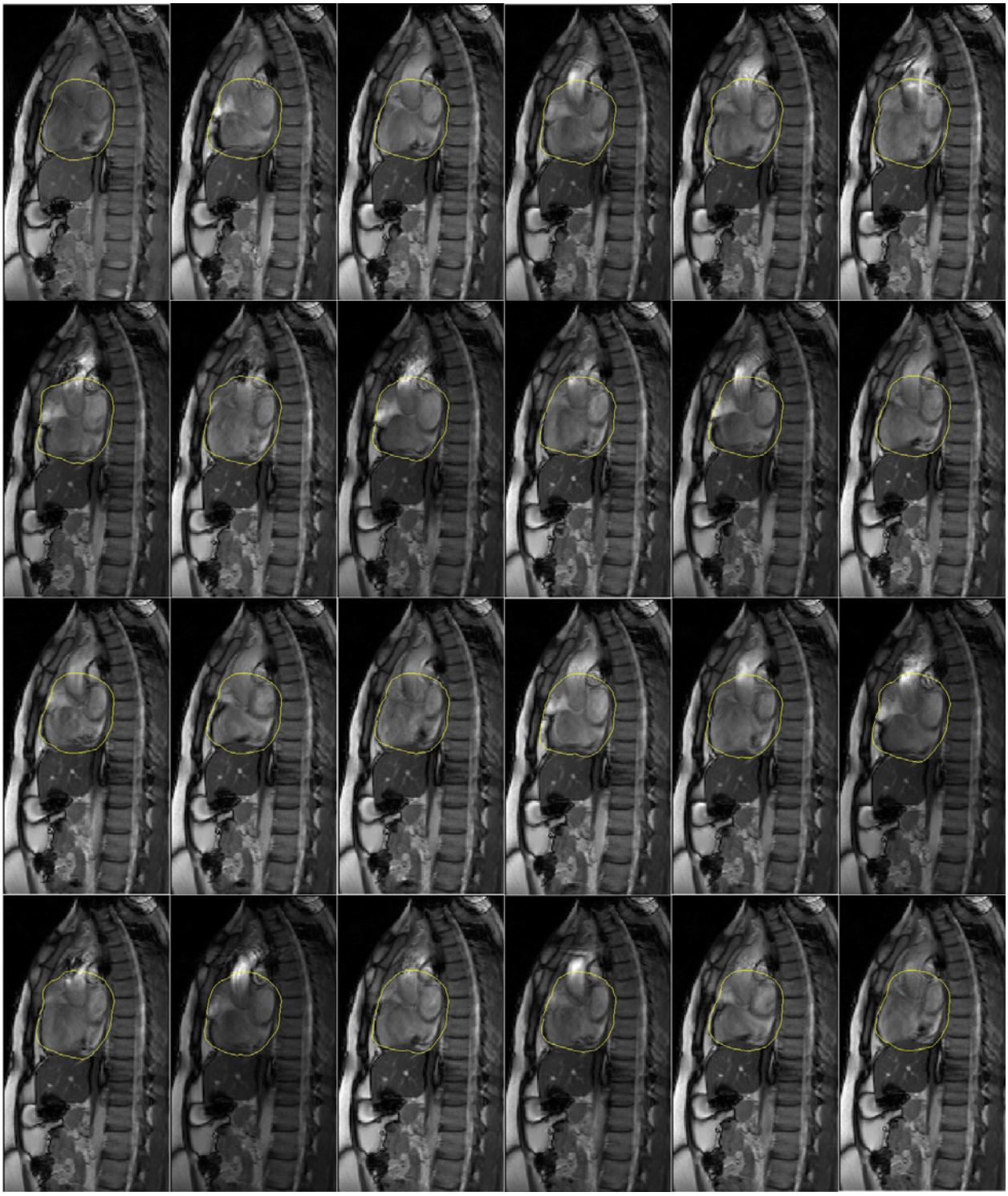

Figure 3.19. M hearts following the real data for some frames of the 12th slice

4. Second technique

Second technique motivation

After finishing the first technique, we have a consistent model of the heart to represent the real movement of the respiration. Now we know where the heart will be at every given respiratory phase, this is to say we can know the heart surface at every operating point.

The next step will be to reproduce an averaged heart, and using the information we get from the M averaged hearts, extract the movement (translation and rotation) of each heart with the averaged heart. Doing this, a translation and 2 rotations will be extracted for every respiratory instant, and what we want to know is if this motion is as good as the first technique to represent the respiratory motion of the heart.

This second technique assumes that the heart has a rigid body movement **[28]**, which means that the M hearts we have from the first technique have similar volumes, and we can find the translation between one heart and the next one looking at the centroids difference. If the volume of 2 consecutive hearts is very different, the centroids will not be a good representation of the translation, and this second technique will be less precise than the first one.

The following steps are needed to get enough results to figure out how good this second technique is when trying to represent the heart motion.

Finding the centroid of each heart

To find the centroids of all the M hearts, the first idea is averaging all of the points to find a centroid for each volume.

$$centroid_k = \sum_{i=1}^{TOT\_POINTS} heart.k(i)$$

Where k is x,y, and z . So we will find the average of all the points of the heart, naming this average the centroid of the heart. TOT_POINTS is the total number of points of the heart.

The next step finding the centroids will be to give more importance to the center slices than to the side ones, meaning that the bigger the area, the more important when finding the centroid. By doing this we effectively weight each slice by its area, and then normalize the result, to give more importance to the slices that have bigger areas, and to give less importance to the small ones.

So the centroids now can be calculated as:

$$centroid_k = \sum_{sl=1}^{NUM\_SLICES} \sum_{i=1}^{SLICE\_POINTS} heart.k(sl,i) * \frac{area(sl)}{mean\_areas}$$

Where *area(sl)* is the area of the slice *sl*, *mean_areas* is the mean of all the areas, *SLICE_POINTS* is the number of points per slice, and *NUM_SLICES* is the number of slices we have for the heart. Of course, *NUM_SLICES*SLICE_POINTS* equals *TOT_POINTS*.

In the following pictures one can see the calculated centroids for different operative points:

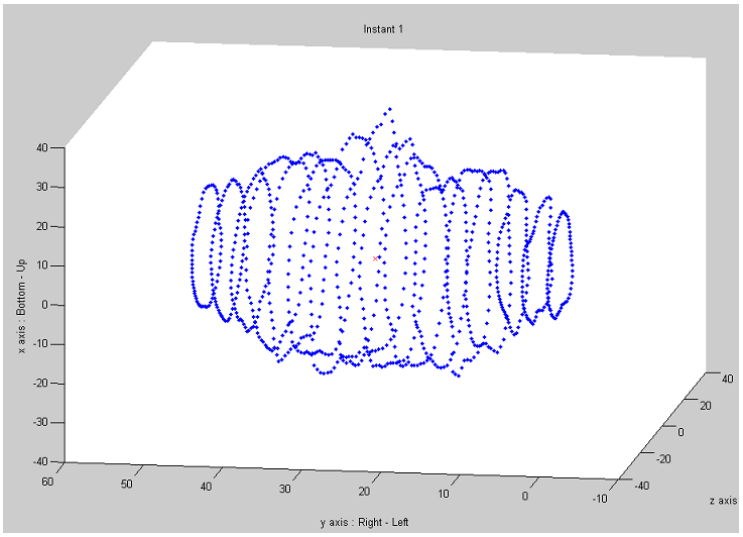

Figure 4.1. Heart in the first operative point, with the centroid represented as a red cross

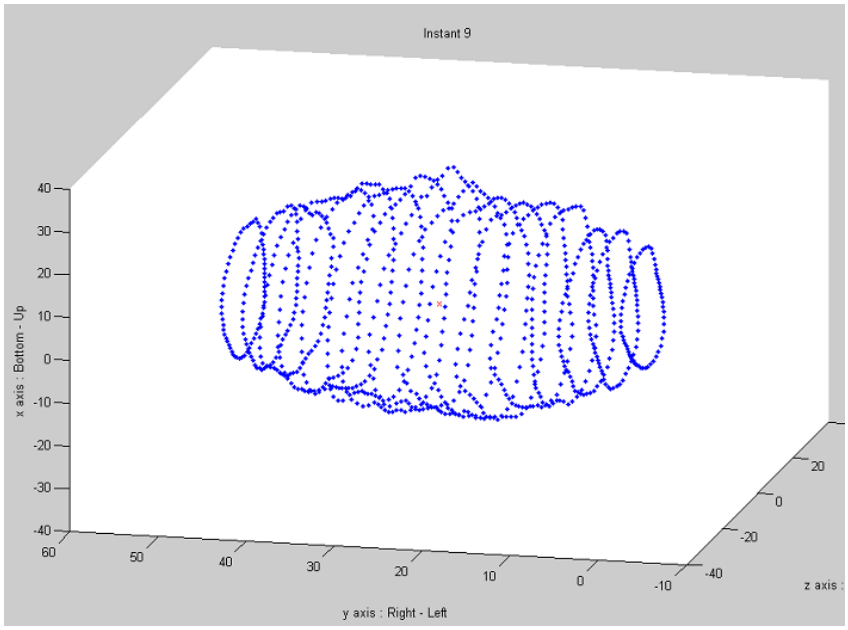

Figure 4.2. Heart and centroid of 9th operative point

Once the M centroids have been calculated, we want to know the movement in the 3 axis, and we want to know if this movement is a good representation of the real respiratory movement.

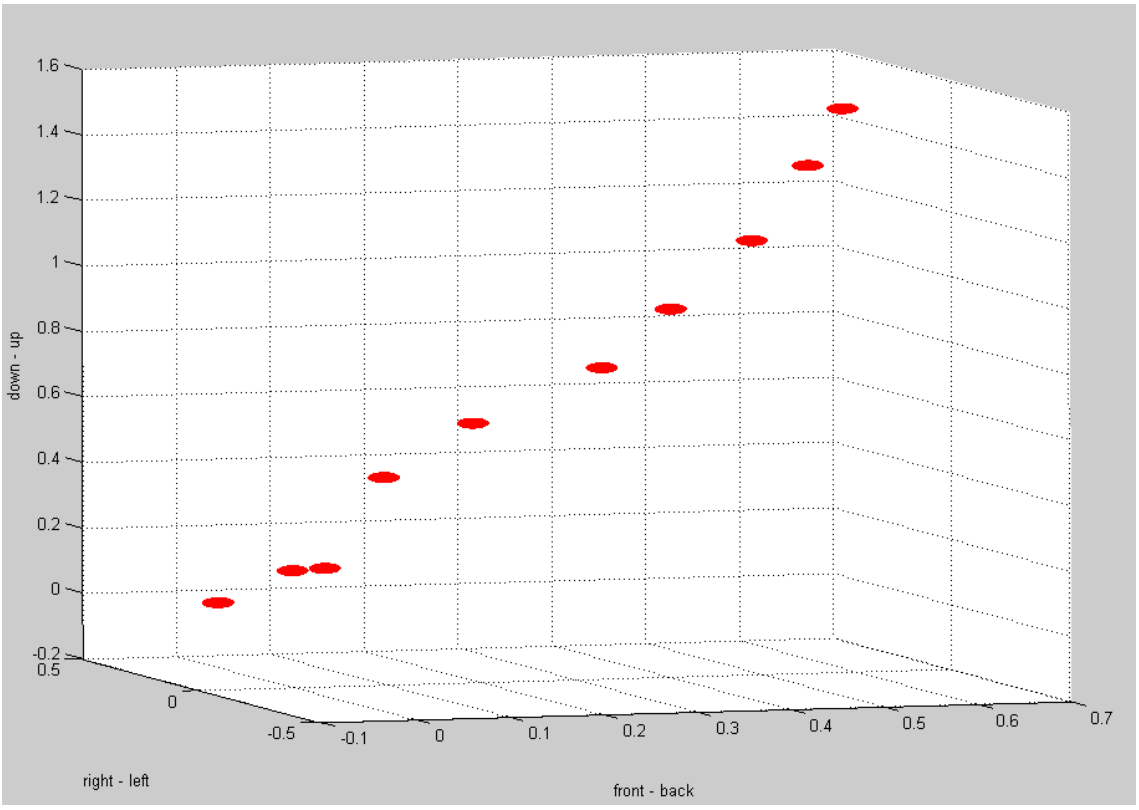

Figure 4.3. Using M=10, the 10 centroids representing the movement of the 10 hearts

Looking at the previous result the first thing one can notice is that the centroids have one big movement in the down-top axis, another important movement in the front-back axis and almost no movement in the right-left axis. This result matches perfectly with the observation, which shows the same 2-axis movement when looking at the respiratory motion.

The second remarkable fact is that the amount of movement in this method is less than the one we had with the first technique. It means that from the lowest phase to the highest one, the up-down movement is around 2 pixels (4mm), when before we had 5 or 6 pixels (10 or 12 mm). In the front-back movement we have less than 1 pixel, meaning less than 2 mm of movement.

Creating the averaged heart of all the M hearts using Spherical Harmonics

The next step to achieve the second technique is to create an averaged heart of M hearts. We want to represent the respiratory motion so we need to have a rigid body to move following the centroid positions calculated in the previous section.

Going back to Chapter I where the Spherical Harmonic theory is explained, the average of the M hearts founded in the previous section will be represented using spherical harmonic functions, and this rigid object will be the representation of the static rigid heart moving due to the respiration.

As one can see in the Spherical Harmonic description, to represent the averaged heart one need to express the radius in function of theta and phi, so all the points must be expressed in spherical coordinates. Then, one can use the values of the radiuses for every theta and phi to calculate the coefficient matrix that represents the entire heart.

The results can be seen in the following images, where the heart is represented with different orders to compare the number of coefficients with the quality of the result:

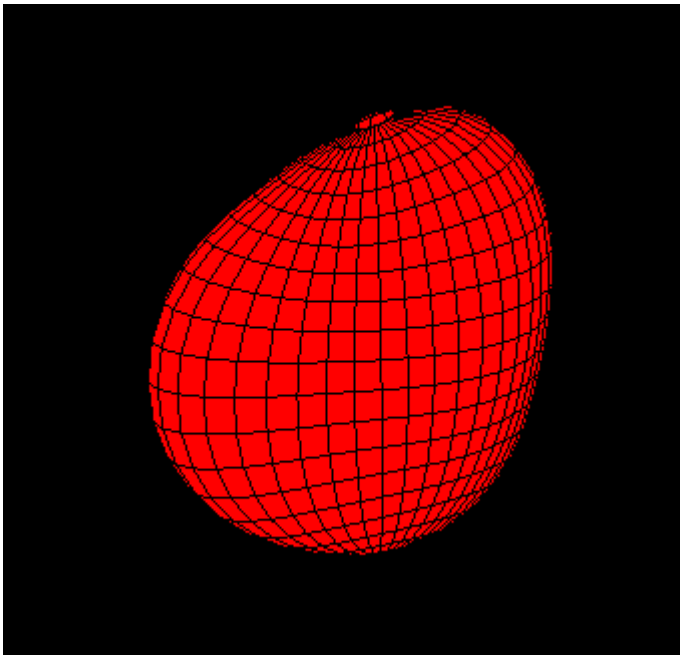

Figure 4.4. Heart reproduced only with order 3.

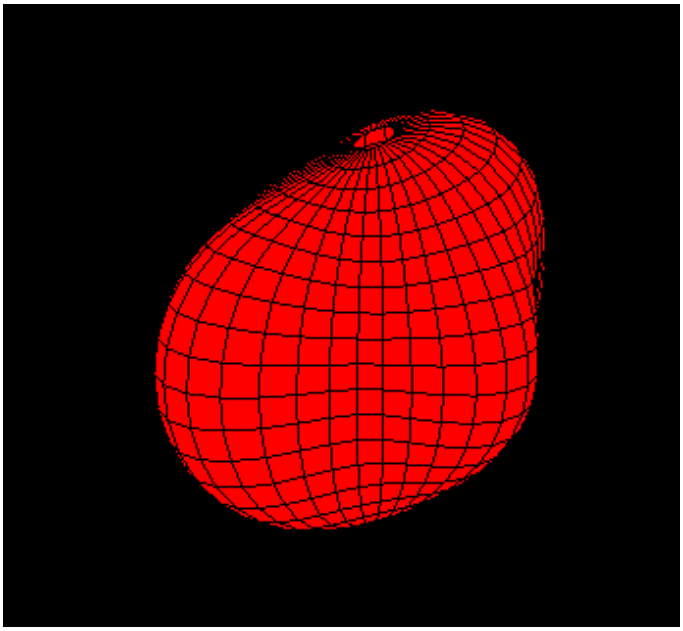

Figure 4.5. Reproduced heart with order 4

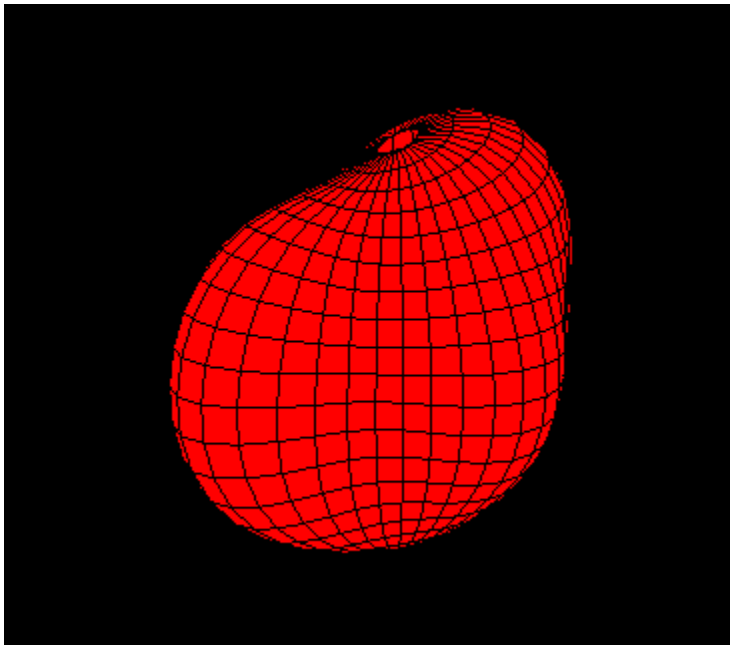

Figure 4.6. Reproduced heart with order 5

We can see that with only a few coefficients the heart is reproduced with a high accuracy. We can use only 4^{th} or 5^{th} order representations to get a good approximation of the averaged heart.

Reproducing respiratory motion using the averaged heart and the centroids

When both the heart and the centroids are reproduced, the respiratory motion can be represented. Taking the original heart and moving it according to the centroids position, the respiratory motion is created:

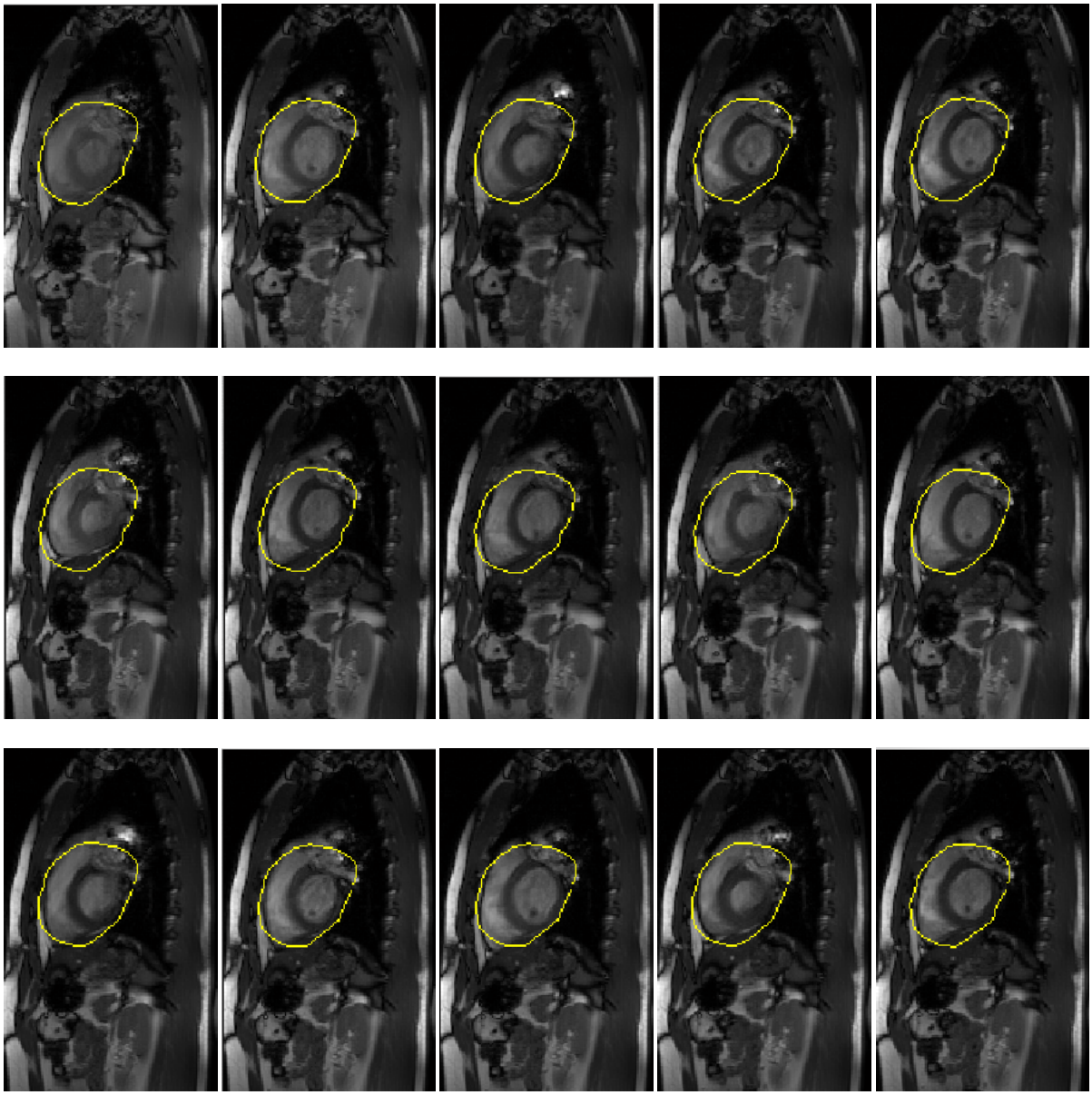

Figure 4.7. Heart moved using the centroid positions following the real data (7^{th} slice)

In the previous figure we can notice that with the second technique the heart has less movement than with the previous technique. What is happening now is that we are using the averaged heart, and we are moving the heart using the centroids. Another example can be useful to understand what is happening.

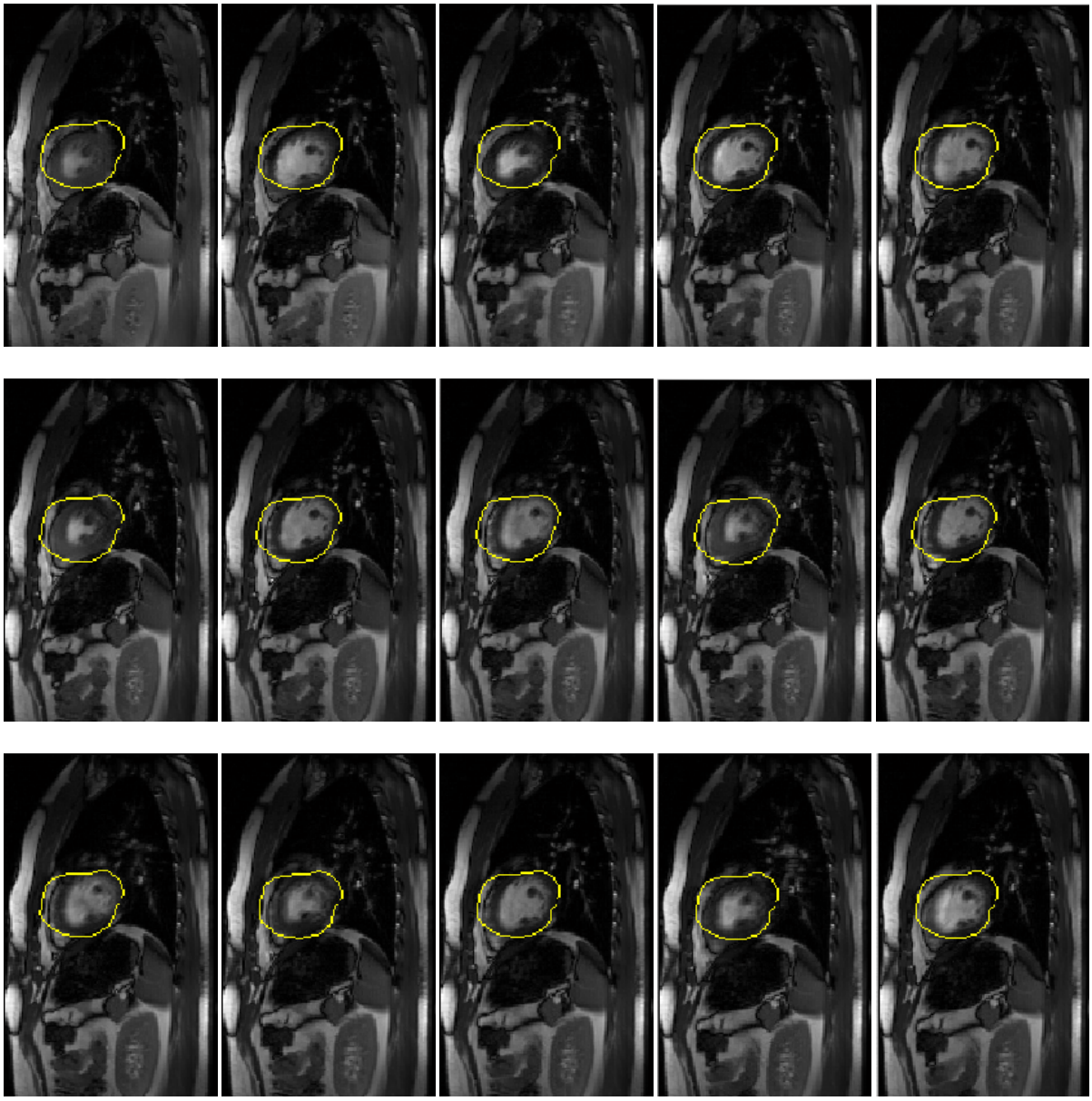

Figure 4.8. Heart moved using the centroid positions following the real data (4th slice)

Adding rotation to the motion

One of the first assumptions we made at the beginning of our work was that the respiratory motion represents both translation and rotation movements **[29]**. Up to this point we have only talked about translation movement, because when one looks at the MRIs we are working with, one can see that the magnitude of translation is much bigger than the rotation. In terms of centimeters, the up-down translation represents between 1 and 2 cm, and the front-back, less than 1 cm. On the other side, the rotation that we can find assuming rigid body motion and using the M recreated hearts is less than 1 degree.

What we do to find the rotation of each respiratory phase is compare the averaged heart with the heart at every phase instant, both having the same centroid, and moving one with a fraction of 0.1 angles per comparison.

$$difference_i = \sum_{k=1}^{NUM\_POINTS} \left\| heart_{orig}(k) - heart_M^i(k) \right\|$$

Where *i* is the rotation used, NUM_POINTS is the number of points of the hearts, and M is the phase instant. Then one must compute the minimum of all the differences, and the rotation that minimizes this difference is the one that better represents the heart.

Then we can add this movement to the translation, and see both movements together, creating the rotation axis to demonstrate the tiny amount of rotation that the heart suffers during breathing:

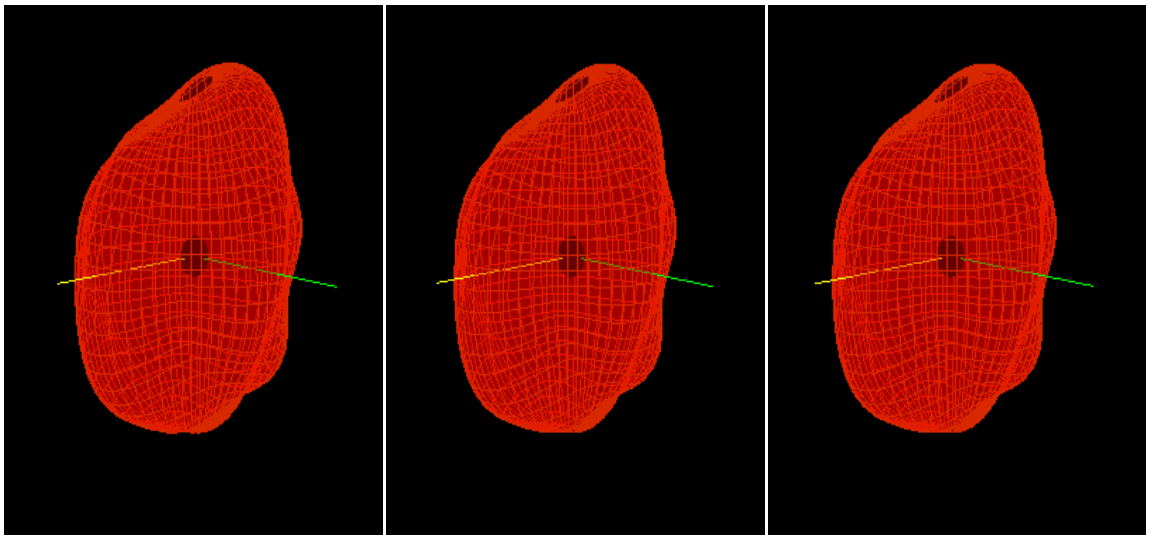

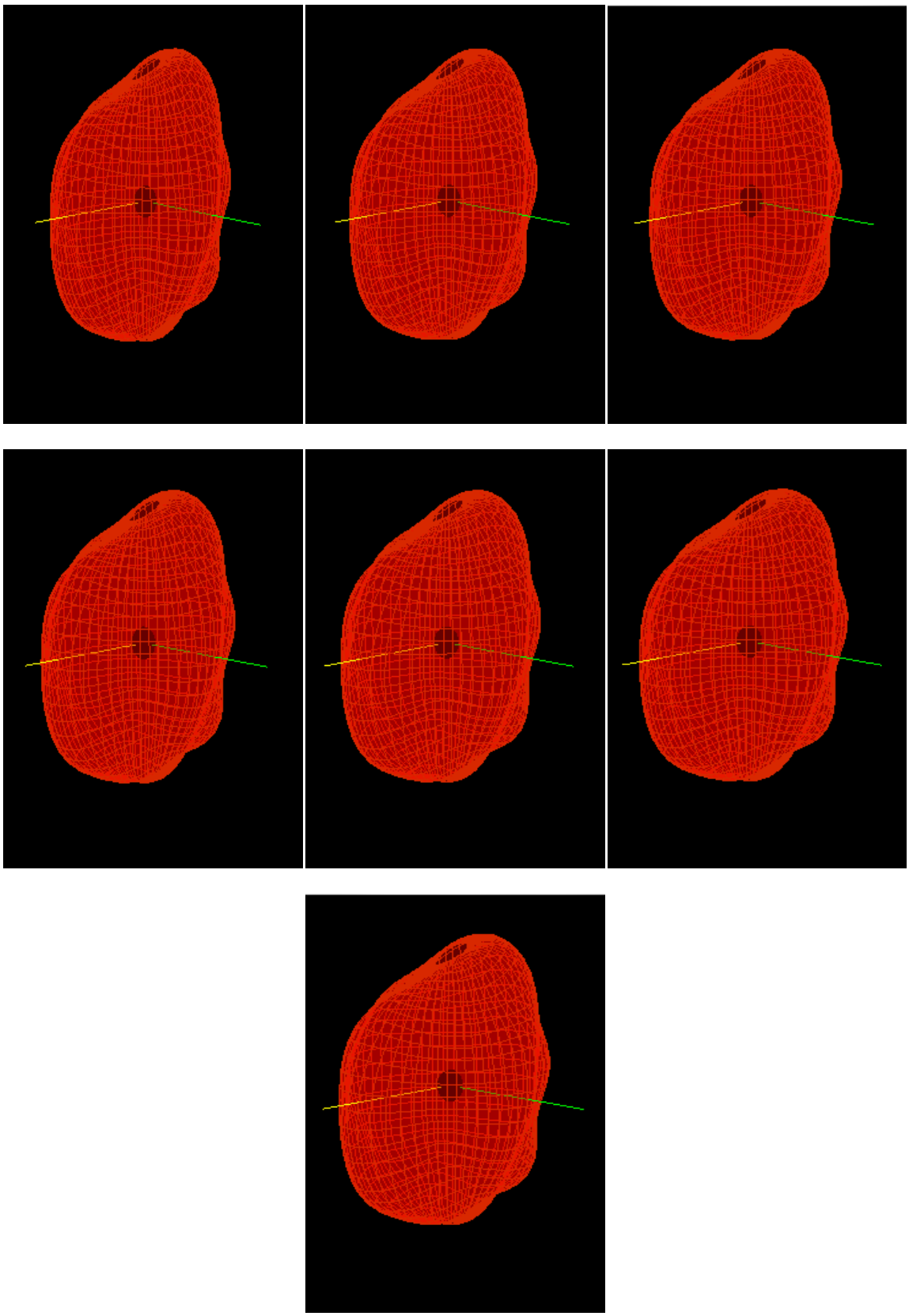

Figure 4.9. Reproduced heart in different respiratory phases.

Checking the results with this second technique

The second technique uses the results of the first one to develop a new respiratory motion. The first technique divides the respiratory cycle in M operating points and creates one heart per point. The second technique assumes that these hearts have a similar volume to model its motion using a rigid heart created as an average of the M hearts, and using the centroids of the M hearts as the translation. In the last section the rotation is added to the motion, using again the M hearts and its minimum differences with the averaged one to calculate the rotations that the heart suffers during the respiratory motion.

The results achieved with this second technique show that the centroids approximation to represent the heart movement is not precise, because the movement of the centroids is smaller than the movement we had with the first technique. This happens because we assumed that the M hearts had a similar volume, so we thought that calculate the centroid of each heart was a good approximation. Probably if we had more samples, this would happen, and it would have a similar volume at every operating point, because in theory if the beating is removed the heart volume doesn't change during its motion.

In the other hand, the results show that the centroids are a good approximation of the movement. The reproduced motion follows the real data correctly, and creates a smooth motion of the rigid heart. Again, the movement direction is correct, but the problem is that the amount of movement is not.

If more samples were used, we could assume that the volumes would be more similar, which means that the centroids would be a better representation of the heart translation. In that case, we would see bigger movement, a movement that could perfectly represent the real respiratory motion.

CHAPTER 4: Discussion and future work

1. Conclusions

This Thesis has briefly presented a review of the current approaches for respiratory motion modeling and discussed the advantages and disadvantages of them. We shortly reviewed the anatomical background and outlined special properties of cardiac MRI data. The successfully achieved goals of this thesis are listed below:

- We have presented the work done using ECG-gated MRIs, extracting the respiratory motion from the images.
- We have developed a method that can track the heart with very little user interaction.
- We have used 2 different techniques to extract the respiratory motion from ungated MRIs.
- With the first technique, we can reproduce the respiratory motion dividing the respiratory cycle and reproducing one heart per operating point.
- With the second technique we assume that the motion can be represented using the heart's centroids, and we reproduce the motion using one heart and moving this heart with the centroid positions.
- We have used spherical harmonic coordinates to represent the heart's shape, and we have seen that less than 50 coefficients are enough to reproduce the heart.

The second chapter presents the work done using DATA1, which is an ECG-gated data. This chapter shows the difficulties one has to focus on when using this kind of data, where the images have very poor temporal resolution. In our work, the only think we can do with this data is extract some information about the respiratory cycle, and after trying different options and techniques, we find that with less than 10 images per cycle it is not possible to reconstruct a respiratory cycle that is irregular. We have two options to increase the temporal resolution. The first one is to make the patient breath slower, and if possible, to beat faster. The second one is break the gating, and have more than one image per beating cycle.

In Chapter 3, we tried to use new data, where the images are not gated to the cardiac cycle. This situation allows us to have more samples per second, but includes the beating motion and deformation of the heart to our images. We developed a method to track the heart with little human intervention, and we extracted the respiratory cycle using a marker included in the new data. Then we divided the respiratory cycle into operating points, and we used the marker to select all the images that have the same respiratory phase. Finally our method created a single heart per every operating point, and this heart was able to follow the real data, and reproduce the respiratory cycle.

At this point we tried to use a second technique that assumes that the heart has a rigid body movement. This is to say that the volume of the heart is the same at every operating point, and the motion is only translation and rotation. If we had more samples, and thus more images to average at every operating point, this assumption would be possible, but as we have less that 5 images (in average) per operating point, the reproduced heart we get at every operating point has not the same volume than the other hearts of other operating points. Because of this reason the results we get with this second technique show a smaller movement than the results from the first technique.

The first thing we notice with the results is that the translation is bigger in 2 directions (right – left and down – up) but is very small in the other direction (front – back). Measuring the centroids of the hearts and looking at the images that show the heart following the real data in Chapter 3, one can notice that the direction of the movement is correct but not the amount of movement. It would be interesting research to check if with more samples this problem disappears or persists.

The second remarkable fact is that rotation is almost non-existent. Again it would be interesting to check if this is due to the small amount of samples we have, or if it is a real movement.

This Thesis shows and checks different ideas when modeling the respiratory motion, with different kinds of MRIs, different approaches, using 2D and 3D data, and also using different techniques. The results obtained reproduce a clear respiratory cycle, and can predict where the heart will be at every respiratory phase with little error. More work can be done in this field, and more data has to be used to develop a complete system to mix both the beating and the respiratory motions.

2. Future work

After months working with different datasets and analyzing the information one can extract of each one, we think that the ungated data is better when modeling the respiratory motion, because it allows more frames per second. In the future work done in this field, the first thing to be done is to have a longer acquisition, this is to say instead of having 50 frames per slice, have 100 or more. This will give more data to the research, and will allow more divisions of the respiratory phase. The fact of having ungated data should mean having also more frames per second, so with both alternatives together, one can have a big amount of data to analyze and to model the respiratory motion.

If the ungated data is chosen (as we recommend), the next step should be to improve the segmentation methods we have used in our Thesis. Our idea was to model the respiratory motion, to study and extract the respiratory cycle, but not to reproduce an exact shape of the heart. Because of this, the method used to track the heart must be improved. With this improvement one will have more realistic data and with less error, which will represent better averages at every operating point, and in general, better results when reproducing the respiratory motion.

As we have fully explained during the Thesis, we have used two different techniques to reproduce the respiratory motion. The first one had good results but included beating motion (the heart was different from one operating point to the next one), and the second one had a tiny translation. This means that more techniques can be used to reproduce the respiratory motion when the data and the respiratory cycle are acquired.

Finally, there is a long path in front of us, using Gearard Pons's Thesis **[3]** and this Thesis to create a complete movement of the heart due to the respiration and the beating. Use both thesis to develop a method to extract the heart's motion will create a real time motion of the heart movement, that can help surgeons to track the catheter position inside the heart, which is the final goal of this project.

References

[1] Crandall MA, Bradley DJ, Packer DL, Asirvatham SJ. *Contemporary management of atrial fibrillation: update on anticoagulation and invasive management strategies*. Department of Internal Medicine, Division of Cardiovascular Diseases, Mayo Clinic, Rochester, MN 55905, USA.

[2] Silva RM, Mont L, Berruezo A, Fosch X, Wayar L, Alvarenga N, Chueca E, Brugada J. *Radiofrequency ablation in the treatment of focal atrial fibrillation using circumferential mapping and segmentary disconnection of pulmonary veins.*

[3] Gerard Pons. *4D Cardiac MRI Segmentation and Surface Reconstruction*. Northeastern University, 2008.

[4] J.D. Dougherty. *The relation of respiratory changes in the horizontal QRS and T-wave axes to movement of the thoracic electrodes*. J. Electrocardiology 1970.

[5] J.D. Dougherty. Change *in the frontal QRS axis with changes in the anatomic positions of the heart*. J. Electrocardiology, 1970.

[6] H.G. Borgen, B.M.T. Lantz, R.R. Miller and D.T. Mason. *Effect of respiration on cardiac motion determined by cineangiography*. Acta Radiologica Diagnosis, November 1977.

[7] Y. Wang, S.J. Rieder and R.L. Ehman. *Respiratory motion of the heart: kinematics and the implications for the spatial resolution in coronary imaging*. Man. Reson. Med., May 1995.

[8] K. McLeish, D.L.G. Hill, D.Atkinson, J.M. Blackall and R. Razavi. *A study of the motion and deformation of the heart due to respiration*. In Proc. Intl. Soc. Mag. Reson. Med., 2002.

[9] Levick JR. *An Introduction to Cardiac Physiology*. 3rd Ed. Butterworth-Heinmann, 1991.

[10] Dee Unglaub Silverthorn. *Human Physiology*. University of Texas.

[11] Richard E. Klabunde. *Cardiovascular Physiology Concepts*. Lippincott Williams & Wilkins, 2005.

[12] http://users.rcn.com/jkimball.ma.ultranet/BiologyPages/M/Muscles.html

[13] Christopher Purcell, Takunori Mashiko, Kazumi Odaka, and Keiichi Ueno. *Describing Head Shape with Surface Harmonic Expansions*. IEEE TRANSACTIONS ON BIOMEDICAL ENGINEERING. VOL. 38. NO. 3, MARCH 1991.

[14] Gregory E. Fasshauer and Larry L. Schumaker. *Scattered Data Fitting on the Sphere*. Mathematical Methods for Curves and Surfaces II, 1998.

[15] M. Mousa, R. Chaine, S. Akkouche and E. Galin. *Efficient Spherical Harmonics Representation of 3D Objects*. Pacific Conference on Computer Graphics and Applications, 2007.

[16] T. Bülow and Kostas Daniilidis. *Surface Representations Using Spherical Harmonics and Gabor Wavelets on the Sphere*. Technical Reports (CIS), University of Pennsylvania, 2001.

[17] E. W. Hobson. *The Theory of Spherical and Ellipsoidal Harmonics*. Cambridge, University Press, 1931.

[18] Zwillinger, D. *CRC Standard Mathematical Tables and Formulae*. Boca Raton, FL.

[19] MATSUDA TETSUYA. *ECG Gating in Cardiac MRI*. Kyoto Univ., Graduate School of Informatics, JPN

[20] K. Nehrke, P. BGrnert. *Study of the Respiratory Motion of the Heart using Multiple Navigator Pulses.* Philips Research Laboratories, Division Technical Systems, Rtintgenstrasse 24-26, D 22335 Hamburg, Germany.

[21] B. Olbrich, J. Traub, S. Wiesner, A. Wichert, H. Feussner, N. Navab. *Respiratory Motion Analysis: Towards Gated Augmentation of the Liver*. Institut für Minimal-invasive therapeutische Interventionen (MITI), Klinikum Rechts der Isar, Technische Universität München.

[22] Guy Shechter, Cengizhan Ozturk, Jon R. Resar and Elliot R. McVeigh. *Respiratory Morion of the Heart From Free Breathing Coronary Angiograms*. IEEE TRANSACTIONS ON MEDICAL IMAGING, 2004.

[23] V.F. Pisarenko. *The Retrieval of Harmonics from a Covariance Function*. Geophysics J. Roy. Astron, 1973.

[24] G. Bienvenu and L. Kopp. *Optimality of high resolution array processing using the eigensystem approach*. Acoustics, Speech and Signal Processing, 1983.

[25] R.O. Schmidt. *Multiple Emitter Location and Signal Parameter Estimation*. IEEE Trans. Antennas Propagation 1986.

[26] Helmuth Spath, Two *Dimensional Spline Interpolation Algorithms*, AK Peters, Ltd. 1995.

[27] John J. Shynk, *Adaptive IIR Filtering*, IEEE ASSP MAGAZINE, 1989.

[28] Kate McLeish, Derek L. G. Hill, David Atkinson, Jane M. Blackall, and Reza Razavi. *A Study of the Motion and Deformation of the Heart Due to Respiration*. IEEE TRANSACTIONS ON MEDICAL IMAGING, VOL. 21, NO. 9, SEPTEMBER 2002.

[29] Ivan G. Buliev, Cristian T. Badea, Zoi Kolitsi, and Nicolas Pallikarakis. *Estimation of the Heart Respiratory Motion With Applications for Cone Beam Computed Tomography Imaging: A Simulation Study*. IEEE TRANSACTIONS ON INFORMATION TECHNOLOGY IN BIOMEDICINE, VOL. 7, NO. 4, DECEMBER 2003.